OBJECTIVE ANALYSIS AND NUMERICAL FORECASTING OF AN EXPLOSIVE DEEPENING CYCLONE USING PRE-OPERATIONAL HIRLAM SYSTEMS

Bennert Machenhauer
The HIRLAM Project c/o Danish Meteorological Institute
Lyngbyvej 100, DK 2100 Copenhagen Ø

1. INTRODUCTION

1.1 The HIRLAM Project

The HIRLAM (High Resolution Limited Area Modelling) project is a joint research and development project among the Nordic Countries and the Netherlands. The main objective of the project is to develop an operational high resolution data-assimilation and forecast model system to be utilized for short range forecasting by the participating countries.

At present the project group consists of 13 scientists of which 4 are working only half time on the project. About half of the scientists are working in a central group hosted by the Danish Meteorological Institute (DMI) in Copenhagen, and the rest are working at their home institutes, the Finnish Meteorological Institute (FMI), the Norwegian Meteorological Institute (DNMI), the Swedish Meteorological and Hydrological Institute (SMHI) and the Royal Dutch Meteorological Institute (KNMI).

The project started in September 1985 and is ending in August 1988. The main pre-operational tests of alternative modules of the final system are planned to take place during 1988.

1.2 The September case: An explosive deepening extratropical cyclone

So far only a limited number of real cases have been used in the HIRLAM development work. During the pre-operational test-period many more cases will be included.

The most extensively used case in the initial tests and experiments is a case from 4-7 September 1985, when an eastward moving cyclone suddenly developed explosively over the North Sea. The DMI surface "hand" analysis from 6 September 00 UT, when the central pressure of the cyclone was close to its minimum value, is shown in Figure 1. The path of the center during the preceding day is indicated on the figure. The cyclone caused severe damage in Denmark due to high winds. Mean winds up to 20-25 ms^{-1} and gusts above storm strength were observed. High precipitation rates caused severe problems due to floods in Sweden and due to snow over the high grounds in Norway.

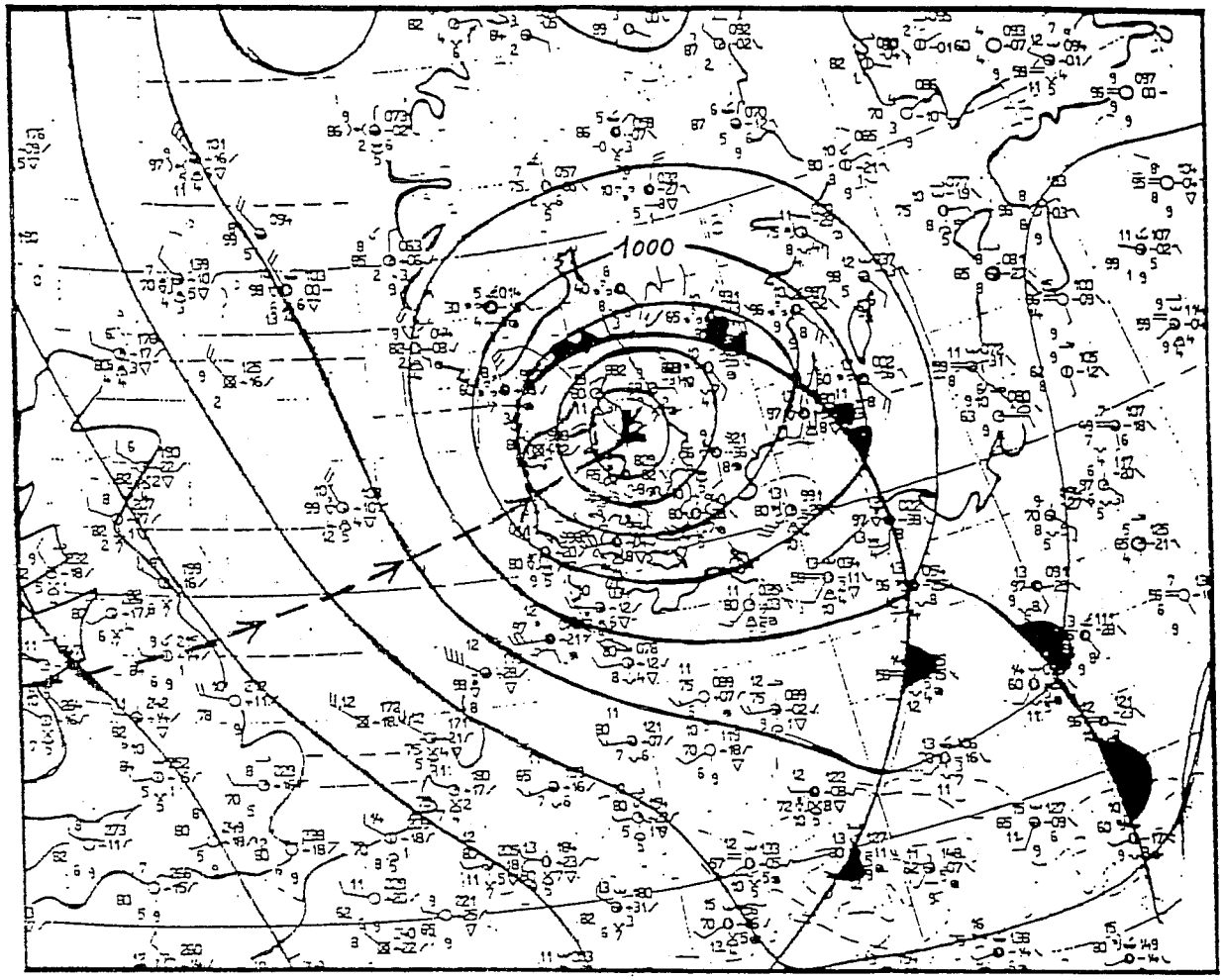

Fig. 1 DMI `hand` analysis, 6 September 1985 00 UT. MSL pressure (5 hPa intervals) and fronts. Path of cyclone indicated.

The sudden development was not forecasted particulary well by operational numerical models and consequently warnings were issued too late by the Nordic meteorological Services. Some operational forecasts, available at DMI, in the morning of the 5th September, when the weather forecast for the following day should be made, are shown in Figure 2. As measures of the quality of the forecasts we shall use the following three numbers:

$$P_c^p - P_c^o, \quad |\vec{r}_c^{\,p} - \vec{r}_c^{\,o}| \quad \text{and} \quad G_{max}^p / G_{max}^o$$

where P_c , r_c and G_{max} are the central pressure, the radius vector to the center and the maximum MSL pressure gradient in the neighbourhood of the low, respectively, and where the superscript o and p indicates observed and predicted values, respectively. The observed values are taken

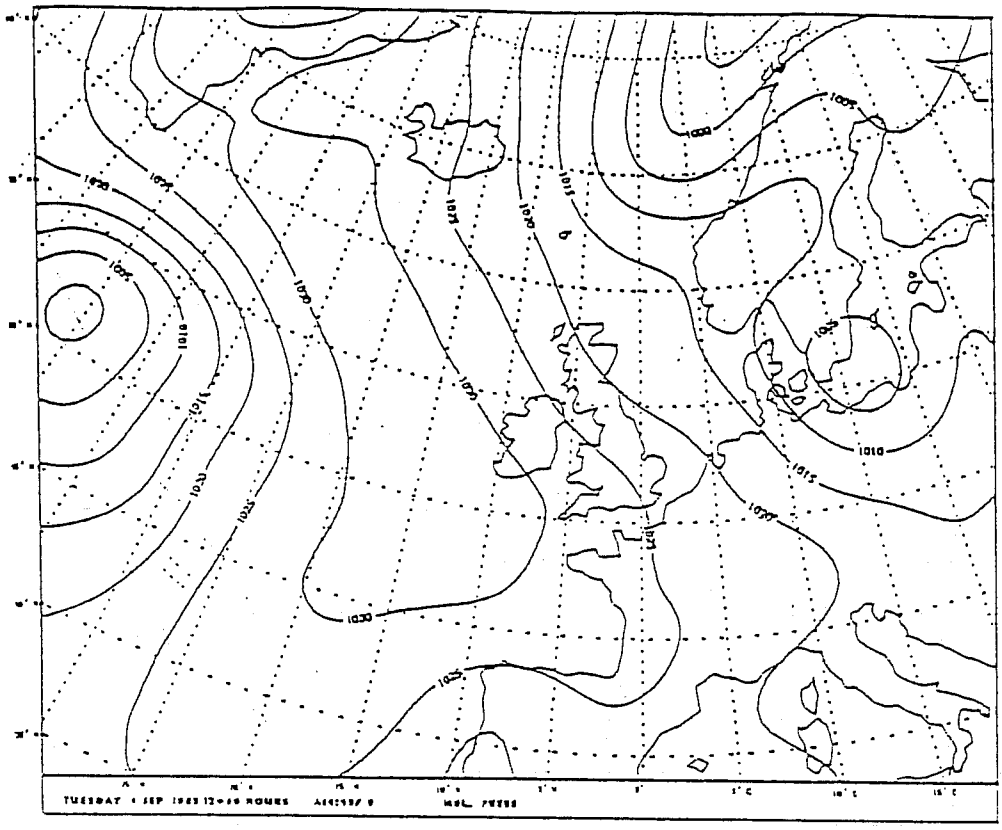

ECMWF 36 hour forecast

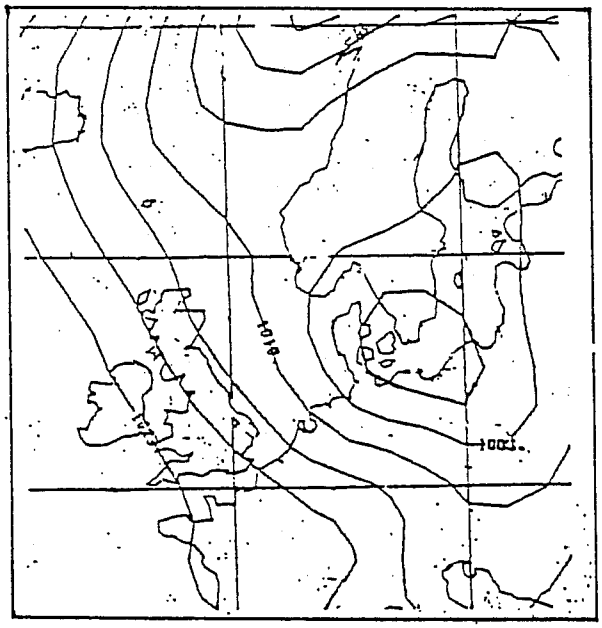

SMHI LAM 30 hour forecast

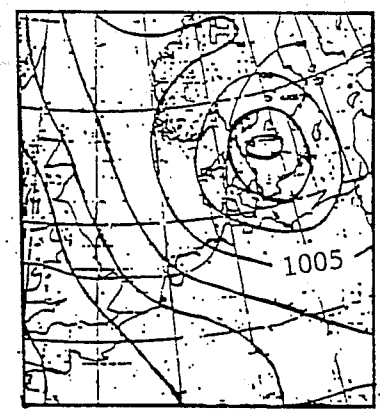

UK LAM 24 hour forecast

Fig. 2 Some operational sea-level pressure forecasts valid at 6 September 1985 00 UT. MSL pressure contour intervals 5 hPa.

from the DMI hand analysis in Figure 1 from which the values P_c^o = 982 hPa and G_{max}^o = 0.1 hPa/km are obtained. The evaluation scores for the three operational forecasts are given in Table 1. We shall use the same measures of quality or verification scores for the experimental forecasts to be presented in the following sections.

Table 1. Verification scores for various forecasts and the baseline objective analysis valid at 6 September 1985 00 UT.

	Evaluation Scores $P_c^f - P_c^o$ (hPa)	$\lvert \vec{r}_c^f - \vec{r}_c^o \rvert$ (km)	$\frac{G_{max}^f}{G_{max}^o}$
ECMWF 36^h forecast (from 4 Sept. 1985 12 UT)	+21	320	0.3
All 36^h forecast (from 4 Sept. 1985 12 UT)	+18	380	0.4
SMHI 30^h forecast (from 4 Sept. 1985 18 UT)	+15	300	0.3
ECMWF 24^h forecast (from 5 Sept. 1985 00 UT)	+12	190	0.4
UKLAM 24^h forecast (from 5 Sept. 1985 00 UT)	+7	180	0.4
All Analysis 6 Sept. 1985 00 UT	+4	0	0.7

It is seen that even the 24 hour UKLAM forecast, with its relatively high resolution (horizontal grid distance ~ 75 km, 15 σ-levels) underpredicts the development of the cyclone, and especially the maximum pressure gradient and hence the surface winds are much too low. Even worse are the 30 hour SMHI LAM forecast (horizontal grid distance ~ 180 km, 9 σ-levels) and the 36 hour ECMWF T106 forecast (equivalent horizontal grid distance ~ 100 km, 16 σ-levels).

In the following we shall present results from some data-assimilation and forecast experiments carried out for the present "September case", using two different experimental HIRLAM systems. The two systems in question are described briefly in Plate 1 and Plate 2, respectively.

1.3 The HIRLAM baseline system

The system described in Plate 1 is the data-assimilation and forecast system used initially by the central group in Copenhagen. We call it the Swedish/Danish (S/D) baseline system as it is building upon the system which became operational in Denmark shortly after the start of the HIRLAM project, and because the main components of this system were borrowed from the operational Swedish system.

The analysis scheme of the HIRLAM S/D baseline system is an improved

version of the original SMHI scheme (Andersson et al., (1986)). Besides an increase of the horizontal resolution of the analysis grid several modifications were made to the scheme available at DMI in order to bring it up-to-date and to enable more small scale features to be represented in the analysis. These modifications are described in detail in Gustafsson et al. (1986). Here and in Plate 1 only the most important ones are summarized. Different versions of the analysis scheme were used in a series of sensitivity experiments. Here we describe the basic version used in the present experiments.

Vertical interpolation of analysis increments was introduced instead of full analysis fields. Furthermore, following Lönnberg and Hollingsworth (1986) we introduced new observational error standard-deviations, five term Bessel function series to represent horizontal forecast error correlations, and new vertical correlation functions.

As in the original SMHI scheme the horizontal resolution of the analysis was permitted to vary with analysis parameter, vertical level and actual data density. At ECMWF variation of resolution is at present modelled by a variation of the scaling radius, R, used in the zero--order Bessel functions. (R is the distance to the first extremum of the largest scale Bessel function). At ECMWF a scaling radius of 3000 km is used for mid-latitude geopotential and streamfunction analysis. In order to permit higher resolution of the analysis than in the ECMWF scheme a reduction of the scaling radius down to one third of this value was used over data rich areas.

With more weight given to smaller scales it seems reasonable to decrease the ratio between observation error variance and forecast error variance. Firstly, because the observation errors should decrease as more small scale features are represented and secondly because the forecast error must be expected to increase with decreasing scale (especially in a grid point model). A simple way to model such a reduction of the variance ratio is by increasing the forecast error standard deviations. We use this technique in our baseline system. Thus, compared to the values of forecast error standard deviation determined for the ECMWF model by Lönnberg and Hollingsworth (1986) we are using values which over land are approximately 2.5 times larger.

As in the original SMHI scheme a fixed geographical variation of the values of forecast error variancies is used in the baseline system, with smaller values over land than over sea.

The baseline initialization scheme is the KNMI non-linear normal mode scheme as implemented by Rattenborg (1985) at DMI. This scheme uses the non-linear balance condition and the iteration scheme introduced by Machenhauer (1977), and it is a modified version of the adoption by Bijlsma and Hafkenscheid (1984) to a limited area model on a lat-long grid. Only adiabatic tendencies from the forecast model are used and two vertical modes are initialized in the baseline system.

The baseline prediction model is the version of the ECMWF semi-implicit

PLATE 1

HIRLAM S/D Baseline System

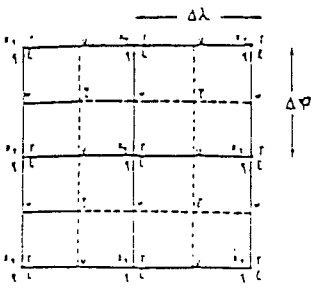

Horizontal (lat-lon) grid (Arakawa type C) and vertical structure of the forecast model

$\Delta\lambda = \Delta\phi = 0.5^{\circ}$

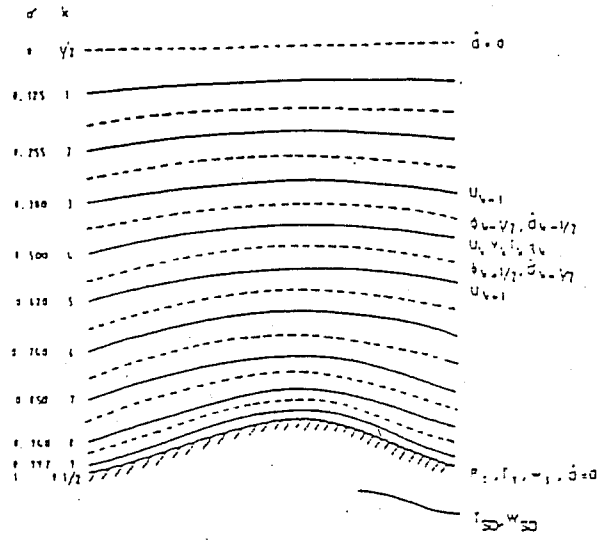

ANALYSIS

Method	3-dimensional uni-variate statistical interpolation with variational adjustment of analysis increments to geostrophic balance (modified SMHI scheme)
Independent variables	λ, φ, p, t
Dependent variables	φ, u, v, r (geopotential, hor.wind, rel.humidity)
Grid	Non-staggered, 10 standard pressure levels
First guess	6 hour forecast (complete prediction model)
Data assimilation frequency	6 hour (±3 hour window)

INITIALISATION

Method	Non-linear normal mode scheme. 2 vertical modes initialized (modified KNMI scheme)

PREDICTION

Independent variables	λ, φ, σ, t
Dependent variables	T, u, v, q, p_s (temperature, hor.wind, mix ratio, surface pressure)
Grid	Staggered in the horizontal (Arakawa C-grid). Uniform horizontal (transformed lat/lon). Non-uniform vertical spacing of levels (see above)
Finite difference scheme	Second order accuracy (ECMWF scheme)
Time-integration	Leapfrog, semi-implicit (Δt = 6 min)
Horizontal diffusion	Non-linear second order scheme with enhanced q diffusion
Earth surface	Albedo, roughness, soil moisture, snow and ice specified geographically. Albedo, soil moisture and snow time dependent
Orography	Smoothed US NAVY mean orography
Physical parameterization	(i) Boundary eddy fluxes dependent on roughness length and local stability (Monin-Obukhov) (ii) Free-atmosphere turbulent fluxes based on mixing length theory (iii) KUO convection scheme (old ECMWF scheme with β and lifting from surface) (iv) Radiation scheme (including clouds), for computing surfaces temperature. Clouds given as a function of relative humidity (v) Stratiform precipitation scheme (critical rel.hum. = 0.8) (vi) Computed land temperature, diurnal cycle included (vii) Climatological sea-surface temperature
Lateral boundaries	Simplified Davis relaxation scheme (Källberg-Gibson), 8 point zone

PLATE 2

HIRLAM Level 1 System

(Preliminary version, September 1987)

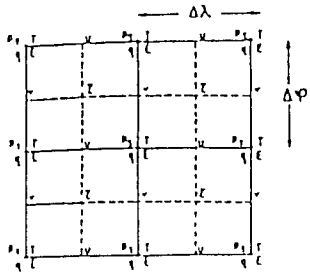

Horizontal (lat-lon) grid (Arakawa type C) and vertical structure of the prediction model

$\Delta\lambda = \Delta\phi = 0.5^{o}$

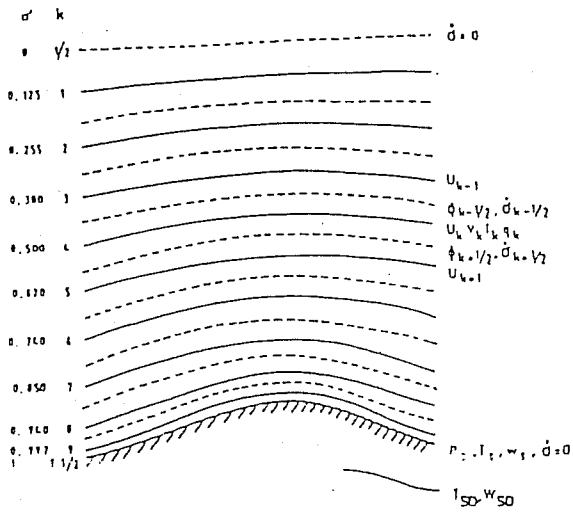

ANALYSIS	
Method	3-dimensional multi-variate statistical interpolation (Limited area version of the New ECMWF scheme with modified parameters)
Independent variables	λ, ϕ, σ, t
Dependent variables	ϕ, u, v, r (geopotential, hor.wind, rel.humidity)
Grid	Non-staggered horizontal grid, vertical levels as prediction model
First guess	6 hour forecast (complete prediction model)
Data assimilation frequency	6 hour (±3 hour window)
INITIALISATION	
Method	Non-linear normal mode initialization. 4 vertical modes initialized. (Modified KNMI scheme)
PREDICTION	
Independent variables	λ, ϕ, σ, t
Dependent variables	T, u, v, q, p_s (temperature, hor.wind, mix ratio, surface pressure)
Grid	Staggered in the horizontal (Arakawa C-grid). Uniform horizontal (transformed lat/lon). Non-uniform vertical spacing of levels (see above)
Finite difference scheme	Second order accuracy (ECMWF scheme)
Time-integration	Leapfrog, semi-implicit (Δt = 6 min)
Horizontal diffusion	Non-linear second order scheme with enhanced q diffusion
Earth surface	Albedo, roughness, soil moisture, snow and ice specified geographically. Albedo, soil moisture, snow and land/sea ice surface temperature time dependent
Orography	Smoothed US NAVY mean orography
Physical parameterization	(i) Boundary eddy fluxes dependent on roughness length and local stability (Monin-Obukhov) (-ECMWF) (ii) Shallow convection (modified Geleyn scheme) (iii) Free-atmosphere turbulent fluxes based on mixing lenght theory (as ECMWF except λ_m = 30 m) (iv) KUO convection scheme (-ECMWF) (i) Longwave and shortwave radiation scheme, diurnal cycle included (HIRLAM). Clouds given as a function of relative humidity (-ECMWF but no convective clouds) (vi) Stratiform precipitation scheme (-ECMWF, except critical rel.humidity = 0.8) (vii) Computed land and sea ice surface temperature, diurnal cycle included (viii) Climatological sea-surface temperature and ice covarage
Lateral boundaries	Simplified Davis relaxation scheme (Källberg-Gibson), 8 point zone

limited area gridpoint model, as implemented and modified by Undén (1982). When implemented at DMI a newer KUO convection scheme, similar to that used in the ECMWF T63 model, was introduced by Rattenborg (personal communication). Except for a reduction of the horizontal resolution and introduction of a new orography no further changes were made to obtain the baseline model.

1.4 The HIRLAM level 1 system

The HIRLAM level 1 system, briefly described in Plate 2, is a first version of the HIRLAM system. It is intended as a starting point for further developments. The system modules described in Plate 2 and in the following are the preliminary versions used in the experiments reported here. Further modifications are planned before the final level 1 system is ready to be used for the first HIRLAM pre-operational tests beginning at the end of January 1988.

The analysis scheme chosen for the level 1 system is a limited area version of the new ECMWF scheme (introduced operationally in May 1986).

A series of experiments has been made with alternative modifications of the ECMWF scheme aiming at the increased resolution of the analysis (Gustafsson and Järvenoja (1987)). In the present version the following modifications were introduced. Firstly, the Bessel function scaling radii used in the ECMWF scheme were reduced by a factor 0.75. At the same time the basic box size and the data search radius were reduced from 660 km to 330 km and from 1500 km to 930 km, respectively. Secondly, the time over which the forecast error variances are growing from the initially estimated values to climatological values was decreased from the value 144 hours used at ECMWF to 36 hours.

The dynamic part of the prediction model is a new version of the S/D-baseline grid point model. The vertical coordinate has been changed to the σ /p hybrid scheme used at present at ECMWF and most of the code has been reorganised and prepared for alternative orthogonal horizontal coordinates. In the present experiments, however, the model is run in a σ -coordinate mode and on a rotated spherical lat-long grid, similar to that used in the experiments with the baseline model. Unlike the base line model the effects of water vapour on density and specific heat capacity are included. The main changes compared to the baseline model are the physical parameterization. A new package developed by the HIRLAM group in Copenhagen has been implemented in the level 1 model. The components of the package are indicated in Plate 2. The present version of the level 1 model is an all-in-core model. It is much more efficient than the baseline model. (The CPU-time is reduced by a factor 3.5 on the ECMWF CRAY XMP computer).

The level 1 initialization scheme is the same as that used in the baseline system, except for changes to σ/p-hybrid coordinates. In the present level 1 version 4 vertical modes are initialised and, as in the baseline version, only adiabatic tendencies are used.

1.5 List of experiments

All experiments described in this note were carried out for the September case, described briefly in Section 1.2. This case was also the main test situation for baseline experiments reported in Gustafsson et al. (1986) and Nordeng and Foss (1987). The limited area grid and the topography used for this case is shown in Figures 3 and 4, respectively.

Table 2. List of data-assimilation and forecast experiments including verification scores of 24 hour forecasts.

Experiment	Resolution (deg.)	Obs. Data Source	Data Assim. Period (date. UT)	Data Assim. System	Initialization Scheme	Prediction model	Lateral Boundary fields	Remarks	Evaluation Scores $p^p_c - p^o_c$ (hPa)	$\lvert \bar{r}^p_c - \bar{r}^o_c \rvert$ (km)	$\frac{c^p_{max}}{c^o_{max}}$
L01	1.0	DMI	4.12-5.00	Baseline (but full field interpol.)	Non-linear bal.eq.	Baseline (Reduced solar heat.)	SMHI Anal.	*) Reduced horizontal resolution	+9	110	0.4
A04	0.5	—	4.00-5.00	—	—	—	—		+4	130	0.5
A11	—	—	3.12-7.00	Baseline	Baseline	—	—		+6	110	0.6
A13	—	—	4.00-5.00	— But *	—	—	—	*) Reduced forecast error variance	+9	180	0.5
A14	—	—	A11 Initial fields			—	ECMWF * Forecast from 4.12	*) Different boundary fields	+7	90	0.6
A09	—	—	3.12-7.00	Baseline (but full field interpol.)	Non-linear bal.eq.	—	SMHI Anal.		+5	100	0.6
F02	—	—	A09 Initial fields			— But *	—	*) New vert. diff. λ_m = 30 m	+6	100	0.5
F04	—	—	A09 Initial fields			— But *	—	*) New vert. diff. λ_m = 160 m	+10	150	0.4
SA1	—	ECMWF	4.00-5.00	Baseline	Baseline	Baseline But *	ECMWF Anal.	*) Increased horizontal diff. (x2.5)	+11	30	0.5
SA2	—	—	SA1 Initial fields			Baseline	—		+6	30	0.6
SA3	—	—	SA1 Initial fields			Baseline But *	—	*) Decreased horizontal diff. (÷10)	0	30	1.0
AA8	—	—	4.00-5.00	Level 1	Level 1	Baseline	—		+4	50	0.7
NT1	—	—	AA8 Initial fields			Level 1 But *	—	*) Without radiation eff. on atm. temp.	+2	80	0.9
NT2	—	—	AA8 Initial fields			Level 1	—		+4	60	0.9

Table 2 summarizes the experiments presented in the following. For each forecast experiment the last column gives the evaluation scores (introduced in Section 1.2) for a 24 hour forecast. The model version used is indicated in the same row in columns 1,7,8 and 9. If a data-assimilation period with the model version in question was made, data base, the data-assimilation period, the analysis scheme used, and the initialization scheme used are indicated in columns 3,4,5 and 6, respectively. If the initial fields were taken from a data-assimilation in which a different forecast model version was used, that model version is indicated.

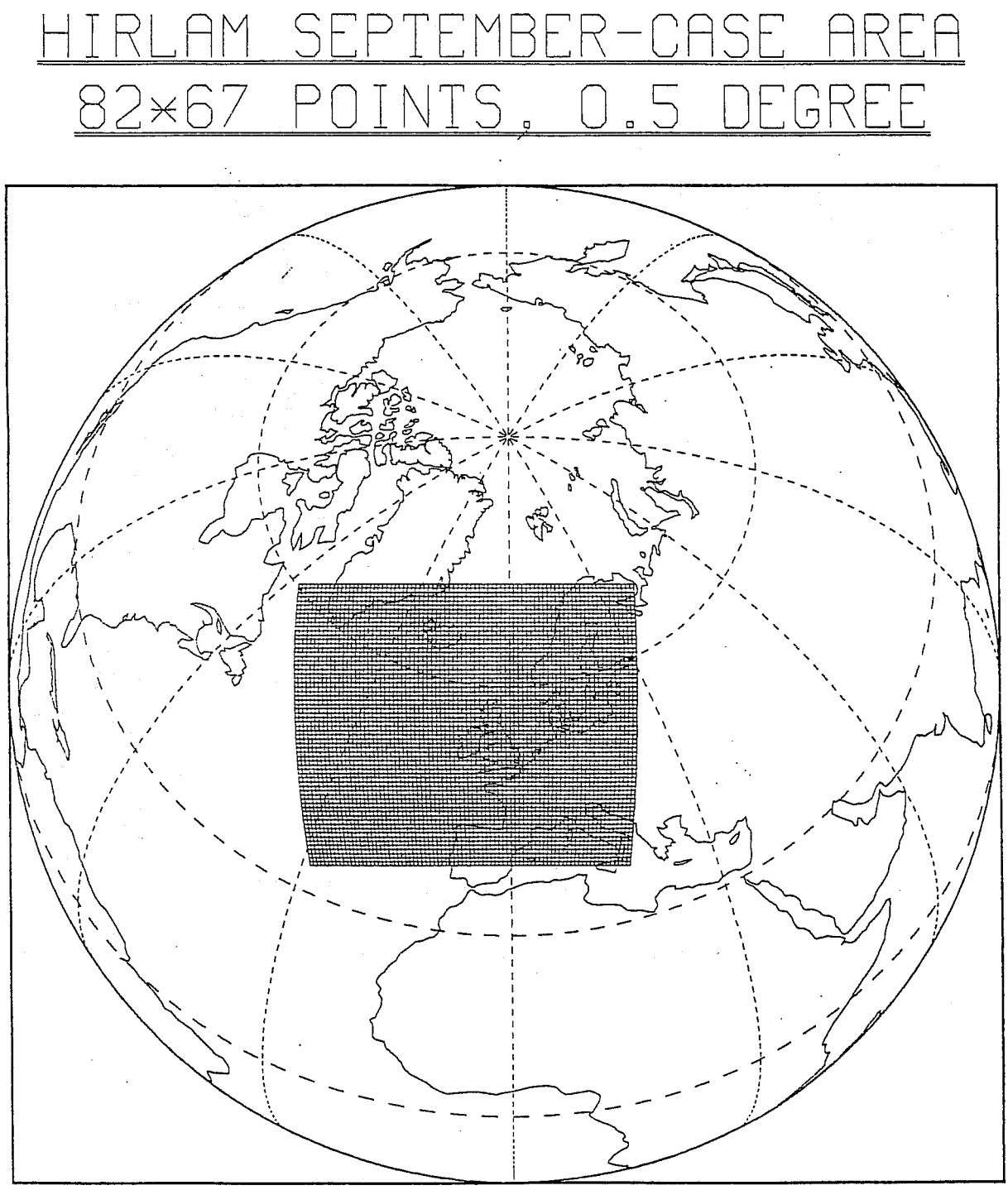

Fig. 3 Limited area grid used in present experiments

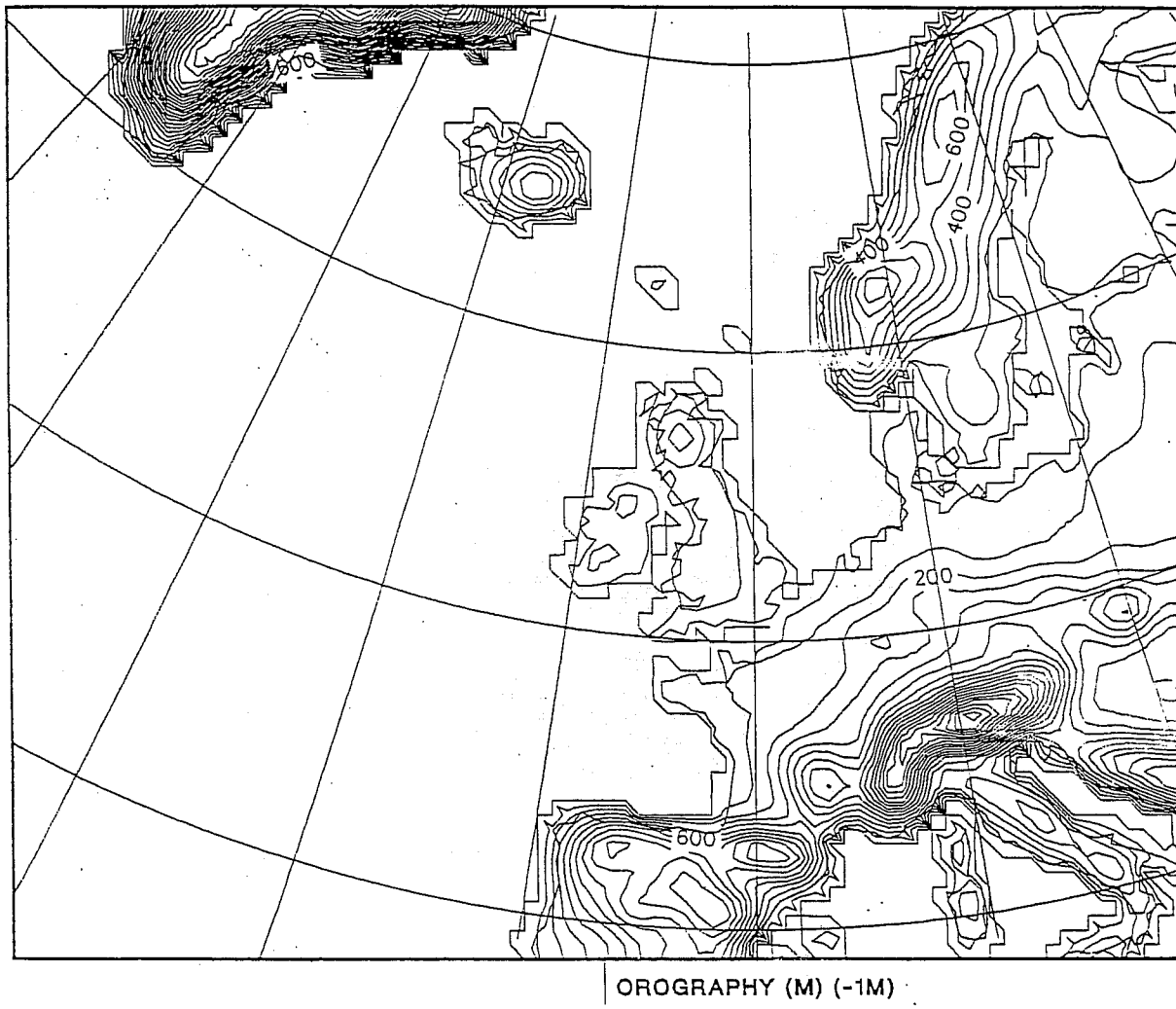

Fig. 4 Topography with horizontal resolution 0.5° x 0.5° used for data assimilation and forecast experiments. Contour interval: 100 m.

Unfortunately, the version of the baseline model used in the first seven experiments of the list had a bug in the code which efficiently reduced the solar radiation used in the surface scheme over land. It is, however, believed that this reduced solar heating of the land surfaces in the present case have had only a minor impact on the results.

2. THE SYNOPTIC DEVELOPMENTS LEADING TO THE EXPLOSIVE DEEPENING OF THE CYCLONE

Figure 5 showns the central MSL pressure of the low as a function of time for two different analyses, the DMI hand analysis (from 5 Sept. 00 UT to 6 Sept. 21 UT) and the baseline objective analysis (A11) (from 4 Sept. 00 UT to 7 Sept. 00 UT). In addition results of some forecasts are shown in the figure. Compared to the hand analysis the objective analysis is seen to overestimate the central pressure near the minimum. Also, the maximum pressure gradient is underestimated in the objective analysis as indicated by the verification scores given in Table 1.

The explosive development is seen to start on the 5th of Sept. 00 UT. An interesting question is why the low suddenly starts to develop at that time. In order to try to answer that question let us start with a look at the development as seen in the baseline objective analysis sequences shown in Figures 6 and 7.

Initially at 4 Sept. 00 Z three surface lows are present on the map. We shall see that all three lows play a role in the development. It is low number 1 (L1) that finally develops explosively when it reaches the North Sea, but the lows L2 and L3 transport cold air southwards ahead and behind the advancing L1 low. Thereby the air mass differences in L1 is sharpened, which then leads to an increased development of the low.

This increase in the air mass differences is shown in the sequence of 850 mb maps presented in Figure 8. When looking at the equivalent potential temperature pattern, it is seen that the frontal zone in the front of L1 collapses with the frontal zone on the southern and western edge of the cold air mass outbreak connected to L2. This collapse happens during the period 4 Sept. 00 UT to 5 Sept. 00 UT. A similar collapse of frontal zones on the rear side of L1 is seen to take place due to the circulation around the occluding low 3. Both processes take place simultaneously and are not completed until 5 Sept. 00 UT, at which time then the sudden increase in available potential energy leads to the explosive development of the L1 low.

3. EXPERIMENTAL FORECASTS WITH THE HIRLAM BASELINE SYSTEM

During the initial HIRLAM development work a series of data-assimilation and forecast experiments with the S/D-baseline system were carried out. A detailed description of these experiments is given in Gustafsson et al. (1986) and Gustafsson and Järvenoja (1987). In the present section some results from these experiments will be presented.

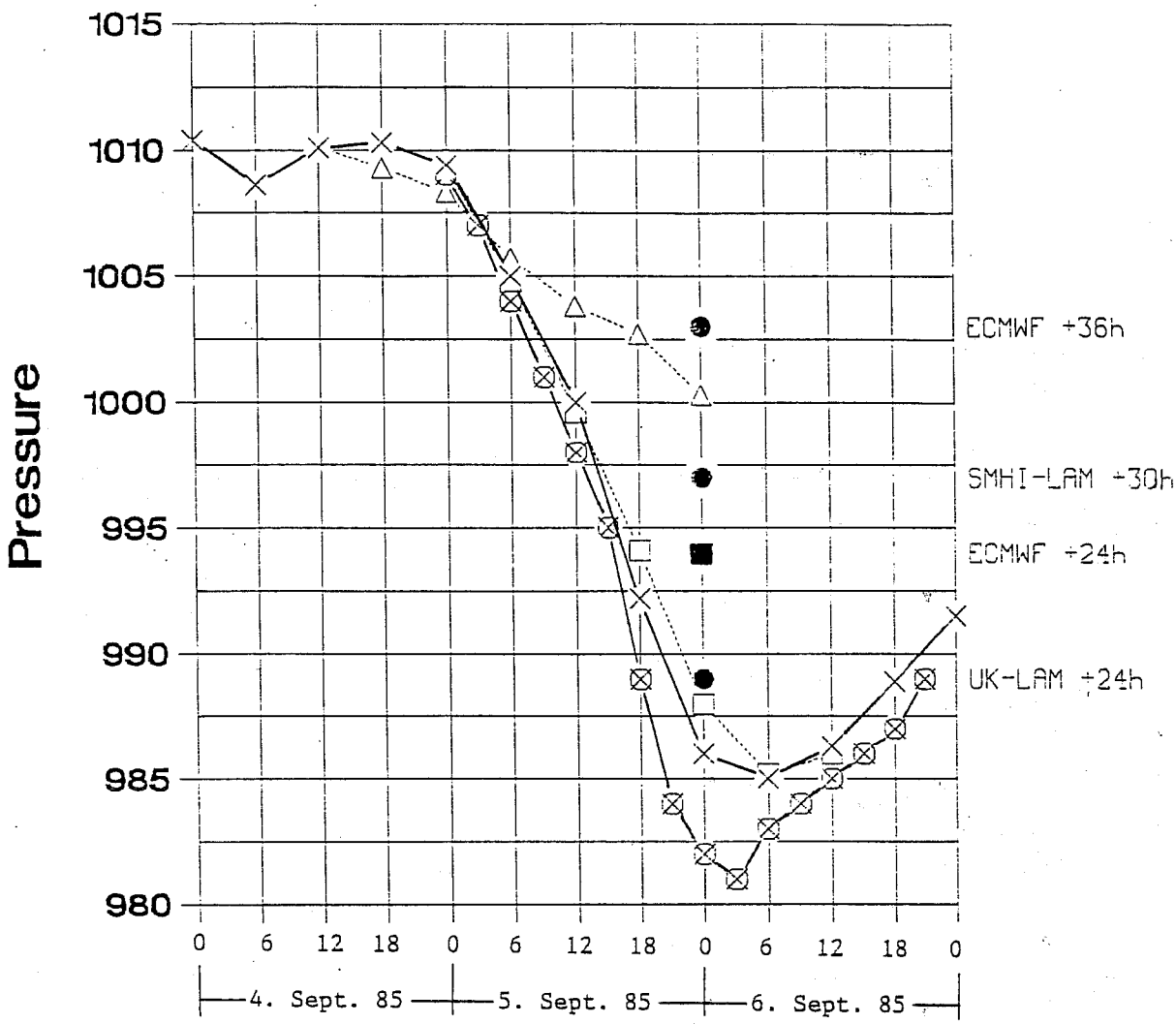

Fig. 5 Central pressure of Low for different analyses and forecasts.

⊠ = DMI hand analysis from 5. Sept. 00Z to 6. Sept. 21Z.

× = All objective analysis from 4. Sept. 00Z to 7. Sept. 00Z.

△ = All 36 hour forecast from 4. Sept. 12Z.

□ = All 36 hour forecast from 5. Sept. 00Z.

● = Operational forecasts from ECMWF, SMHI and UK Met. Office.

■ = ECMWF 24 hour forecast (a rerun from the operational analysis with the T106, L16 model, made available by the Research Department).

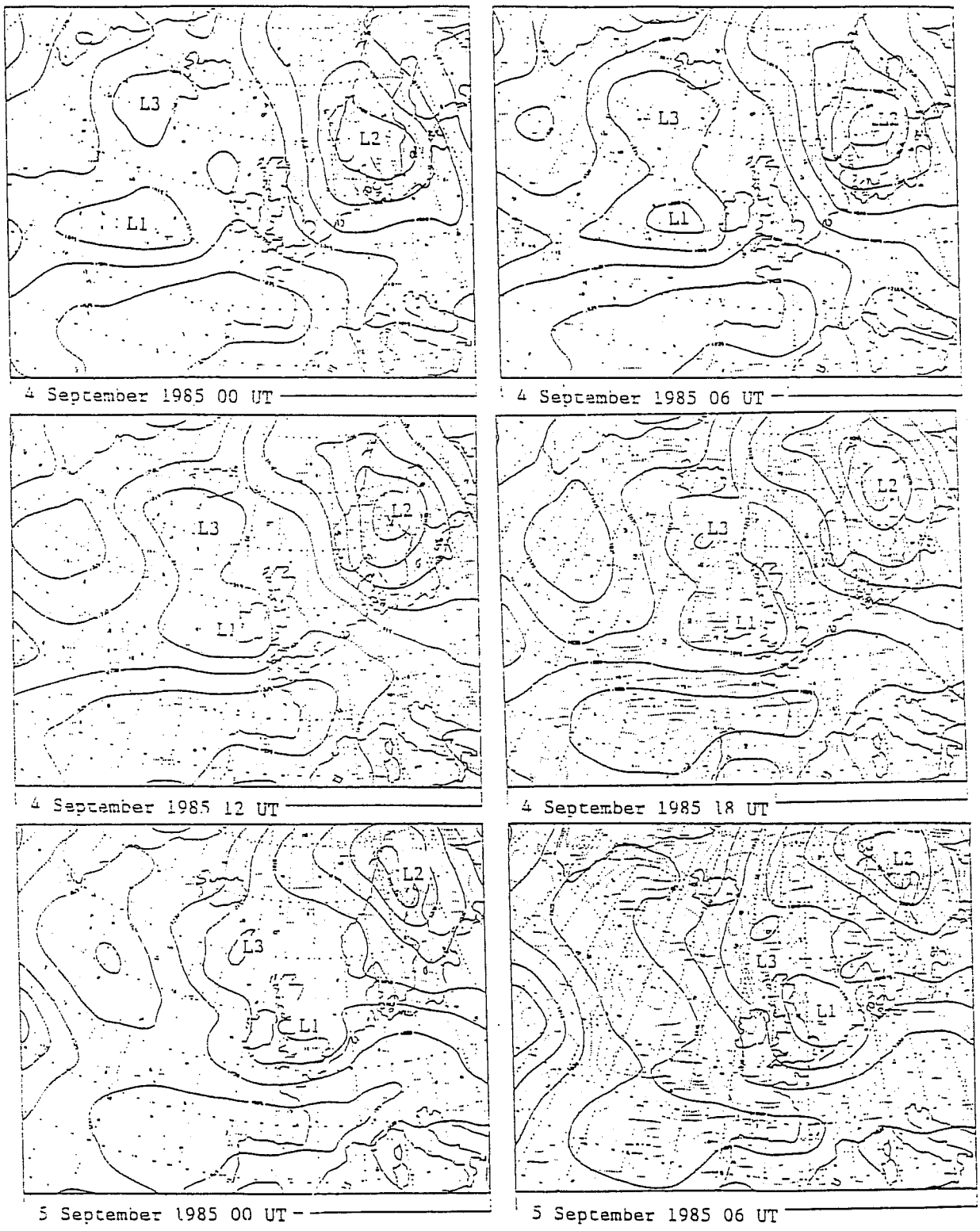

Fig. 6 All MSL pressure analyses from 4 September 1985 00 UT to 5 September 1985 06 UT. Contour intervals 5 hPa

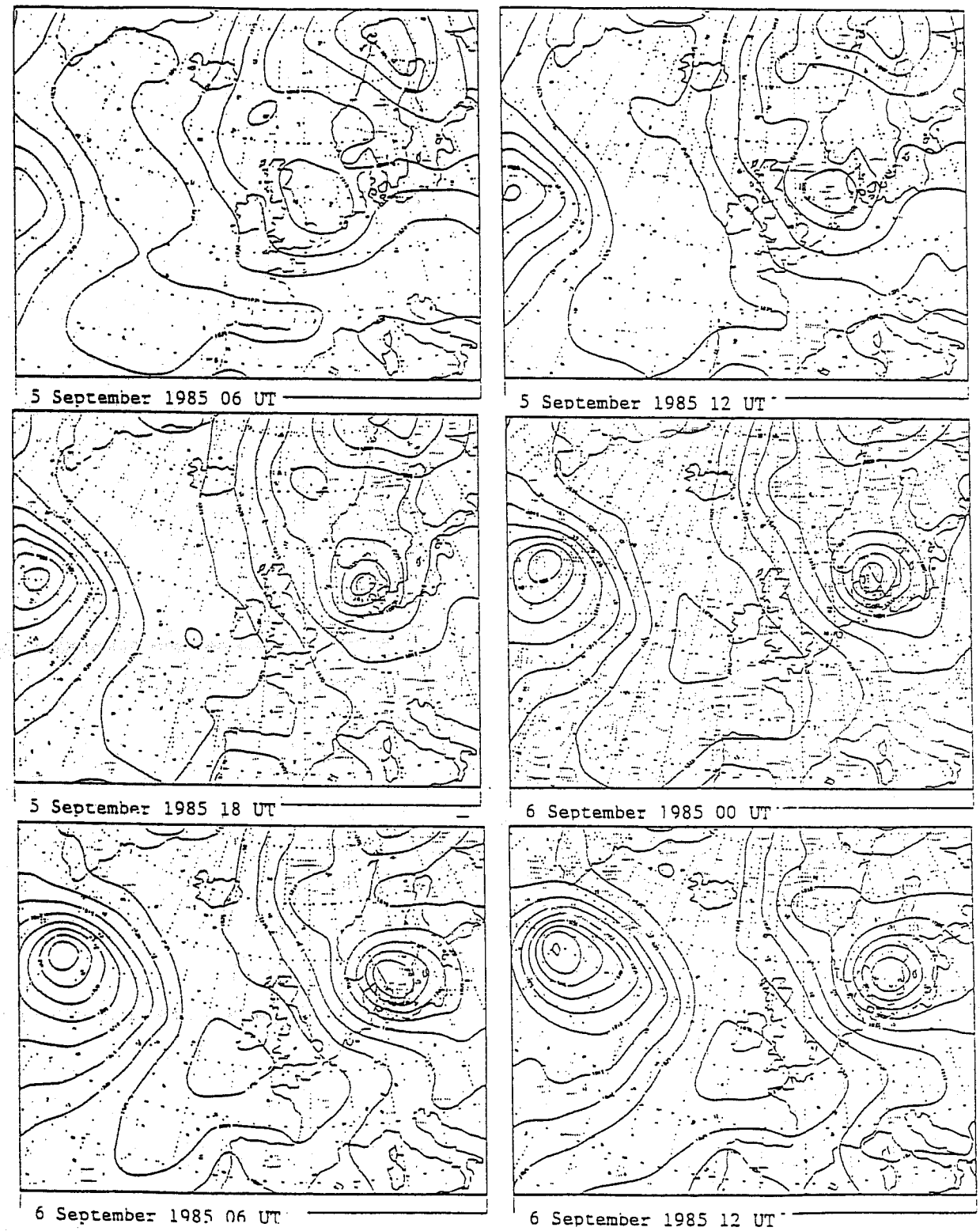

Fig. 7 All MSL pressure analyses from 5 September 1985 06 UT to 6 September 1985 12 UT. Contour intervals 5 hPa

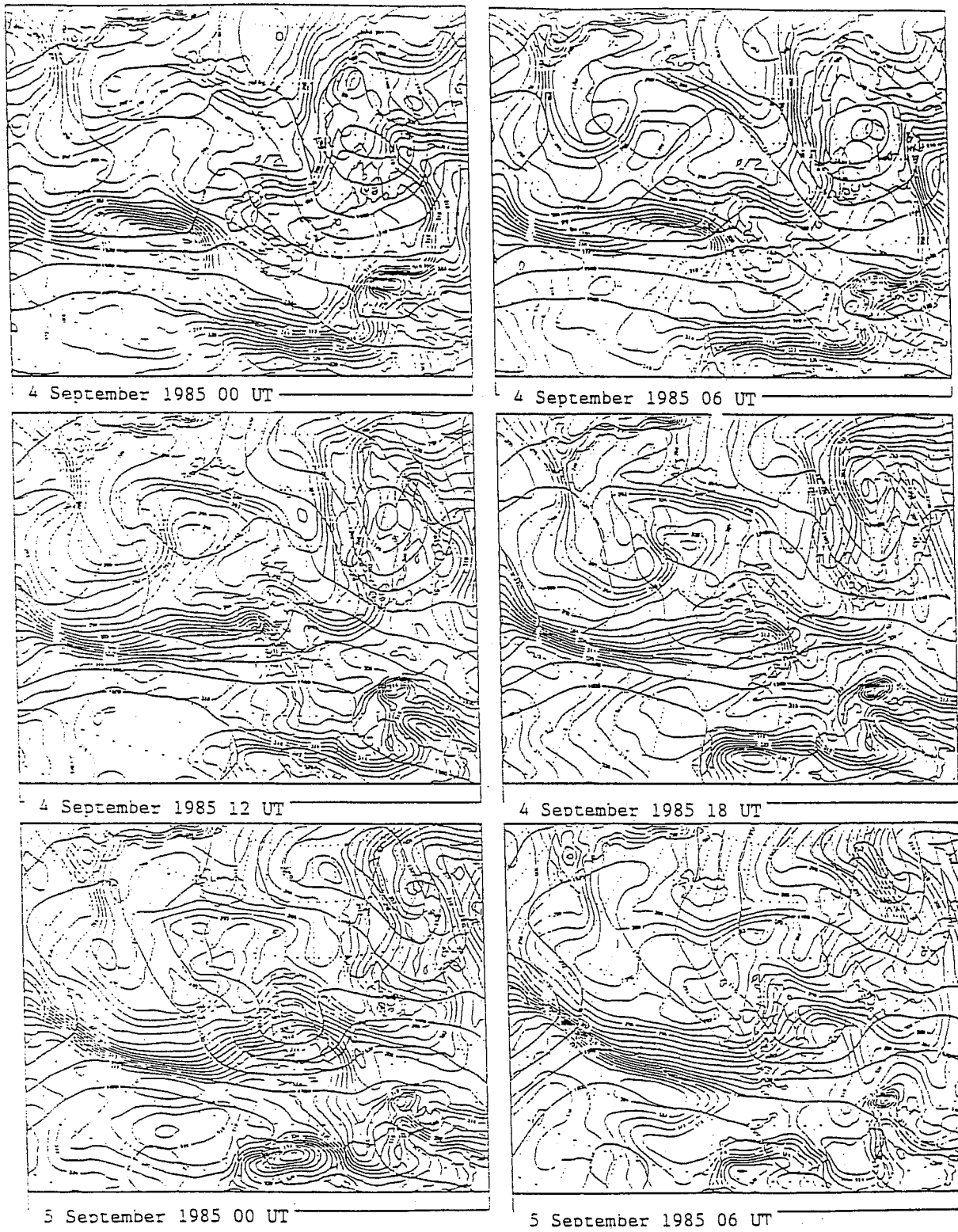

Fig. 8 All 850 hPa analyses. Thick lines height, contour intervals 40 m. Thin lines equivalent potential temperature, contour intervals 2 K

3.1 Sensitivity to the initial state

The difference between the quality of the operational forecasts presented in the sub-section 1.2 (Figure 2 and Table 1) indicates a dependence on forecast length. Especially the 36 hour ECMWF forecast from 4 Sept. 12 UT is surprisingly poor. In order to see if the baseline system with its higher horizontal resolution was able to improve upon that result a 36 hour forecast with initial fields from the A11 data-assimilation was made with the baseline model. The resulting surface forecast valid at 6 Sept. 00 UT is shown in Figure 9 (the verification scores are given in Table 1).

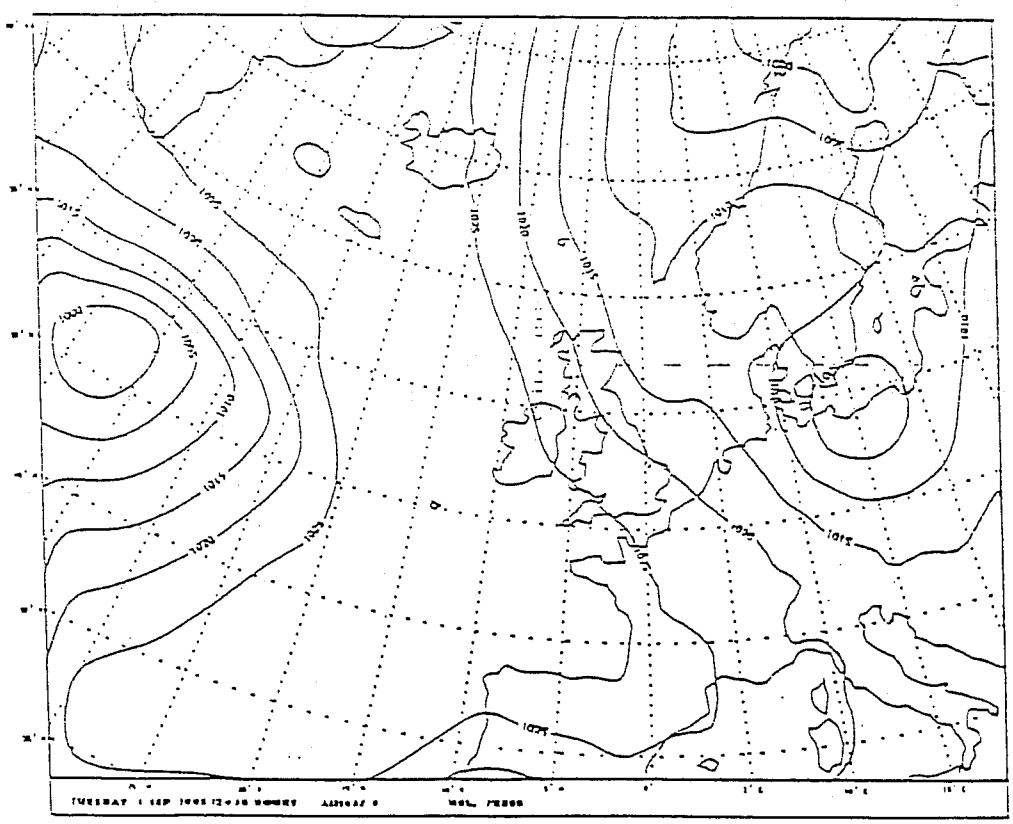

Fig. 9 The A11 36 hour sea-level pressure forecast valid at 6 September 1985 00 UT. Contour interval 5 hPa.

The forecast is seen to be very similar to the 36 hour ECMWF forecast in Figure 2. A possible explanation for the poor results obtained with both systems is errors in the initial analysis due to the location of the two important lows L1 and L2 over the Atlantic Ocean at 4 Sept. 12 UT, (the initial time for both forecasts). It seems likely that the data-assimilation systems, due to insufficient data coverage, are

incapable of producing a sufficiently accurate initial analysis of the baroclinic structures important for the development. For the baseline system at least this is supported by a closer inspection of the changes from one analysis to the next, which shows a pronounced lack of continuity over the Atlantic Ocean (see e.g. Figure 8).

At 5 Sept. 00 UT the Lows L1 and L2 have moved eastward over data rich areas so at that time one should expect to get more accurate analyses. In Figure 10 is shown the 24 hour forecast from 5 Sept. 00 UT with the HIRLAM baseline model (A11) as well as the one with the ECMWF model. The verification scores are given in Table 2 and 1, respectively. Compared to the corresponding 36 hour forecasts in Figure 9 and 2 a clear improvement is obtained.

In the data-assimilation systems two updates of the model fields with observational data have taken place between the analysis at 4 Sept. 12 UT and that at 5 Sept. 00 UT. As only a limited amount of data is available at 4 Sept. 18 UT the main update is that at 5 Sept. 00 UT. The impact of observations in the analysis 5 Sept. 00 UT must therefore be of vital importance, also because the important weather systems at that time are over more data rich areas.

As mentioned in Section 1.3 the impact of observations in the analysis may be changed by changing the values of forecast error variances used in the analysis scheme. It was mentioned also that in the baseline scheme we use values of forecast error variances which are approximately 2.5 times those used at ECMWF. To see the impact of this we made a data-assimilation experiment, A13, in which the values of forecast error variances were decreased to the level used at ECMWF. The 24 hour baseline forecast with initial fields from this assimilation is shown in Figure 11 together with that using the A11 analysis.

A clear deterioration is obtained with the smaller values of forecast error variance. That this is due to a smaller impact of the observations at 5 Sept 00 UT in the A13 assimilation than in the A11 one is illustrated in Figure 12, which shows analysis increments at that time for the two data-assimilations. In the important area along the main frontal zone North-West of Ireland much larger increments, which imply a sharpening of the frontal zone, are seen in the A11 analysis.

3.2 Sensitivity to horizontal diffusion and observational data base used

A data-assimilation and forecast experiment was made with the baseline system in order to see the effect of variations in horizontal diffusion.

The same initial fields were used for three 24 hour forecasts SA1, SA2 and SA3 with different horizontal diffusion coefficients. The common initial fields were determined by a data-assimilation in which the ECMWF observational data base was used and where ECMWF analyses were used as boundary fields in the 6 hour first guess forecasts. In these first guess forecasts the horizontal diffusion coefficient was increa-

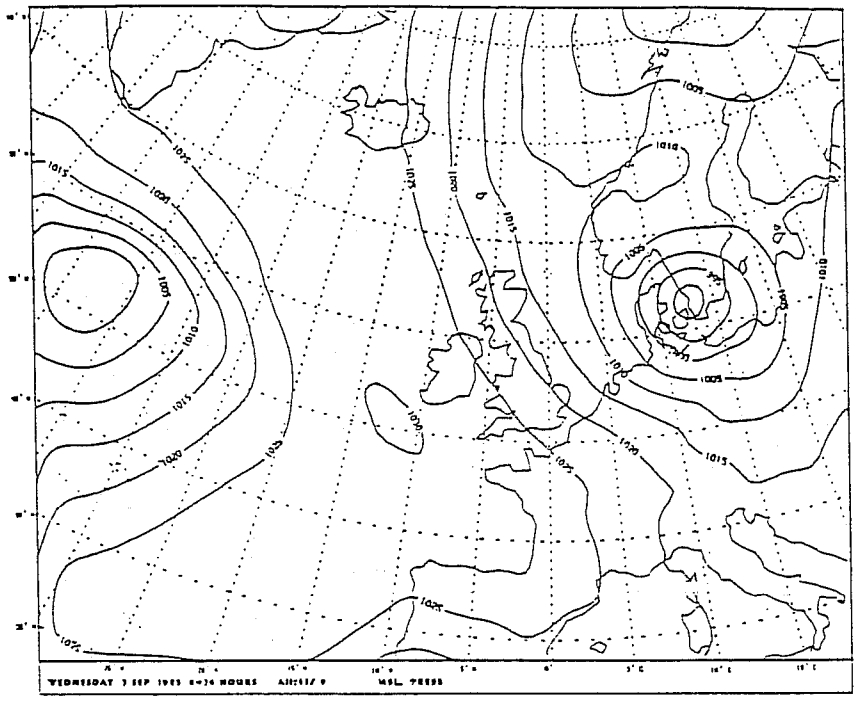

The +24 h sea-level pressure forecast valid at 00 GMT 6 Sept 1985 for experiment A11. Contour interval: 5 hPa.

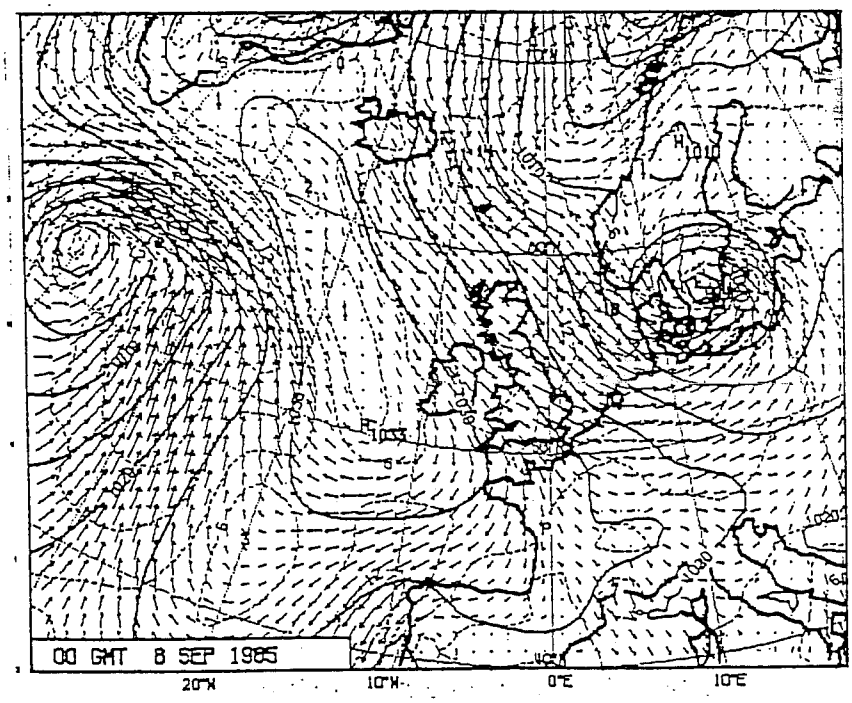

The ECMWF (rerun with T106) +24 h sea-level pressure forecast (together with wind arrows and isotachs) valid at 00 GMT 6 Sept 1985. Contour intervals: 5 hPa for sea-level pressure and 3 m/s for wind speed.

Fig. 10 HIRLAM baseline and ECMWF 24 hour forecasts valid at 6 September 1985 00 UT

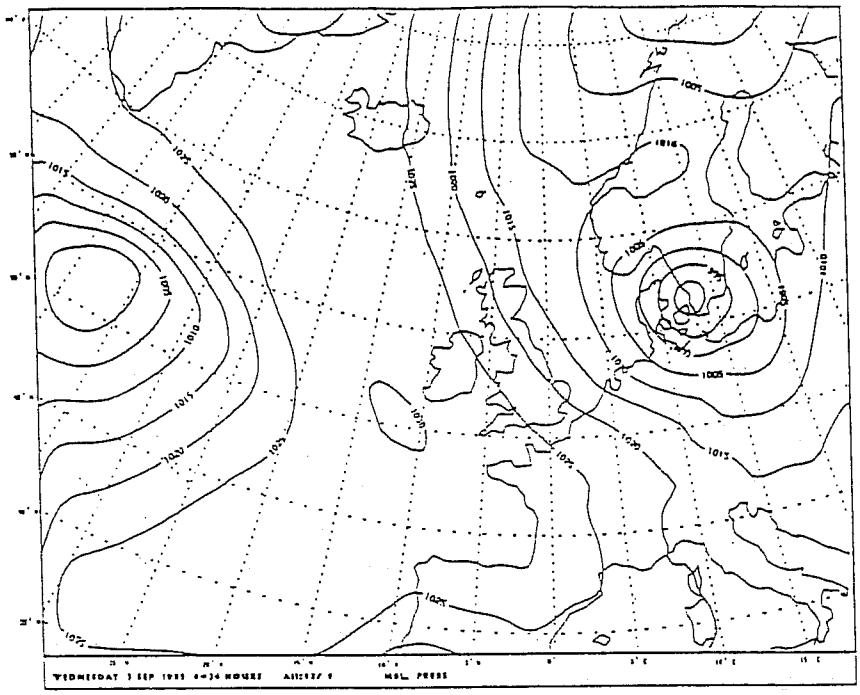

The +24 h sea-level pressure forecast valid at 00 GMT 6 Sept 1985 for experiment A11. Contour interval: 5 hPa.

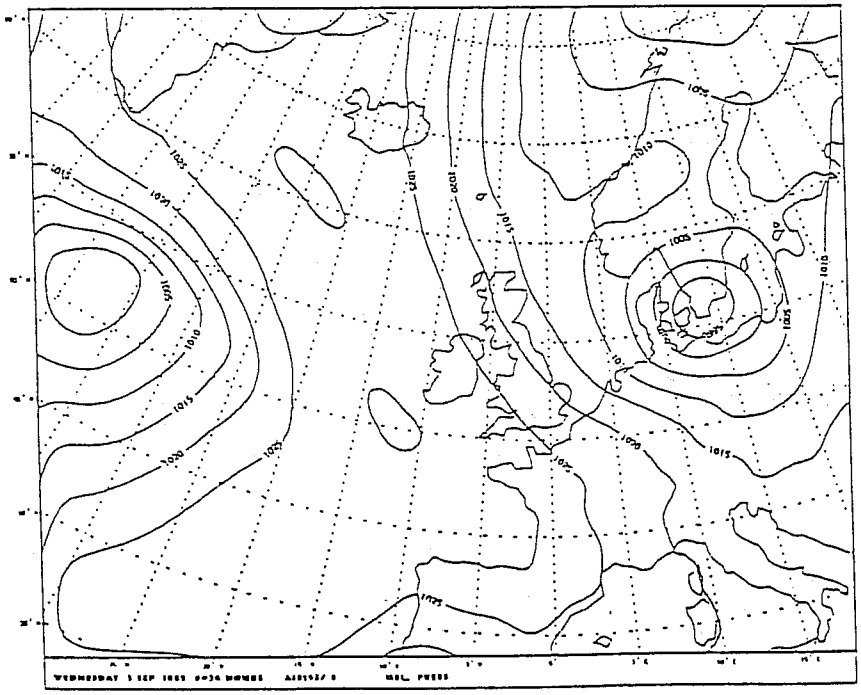

The +24 h sea-level pressure forecast valid at 00 GMT 6 Sept 1985 for experiment A13. Contour interval: 5 hPa.

Fig. 11 HIRLAM baseline forecasts with initial fields from data-assimilations A11 and A13

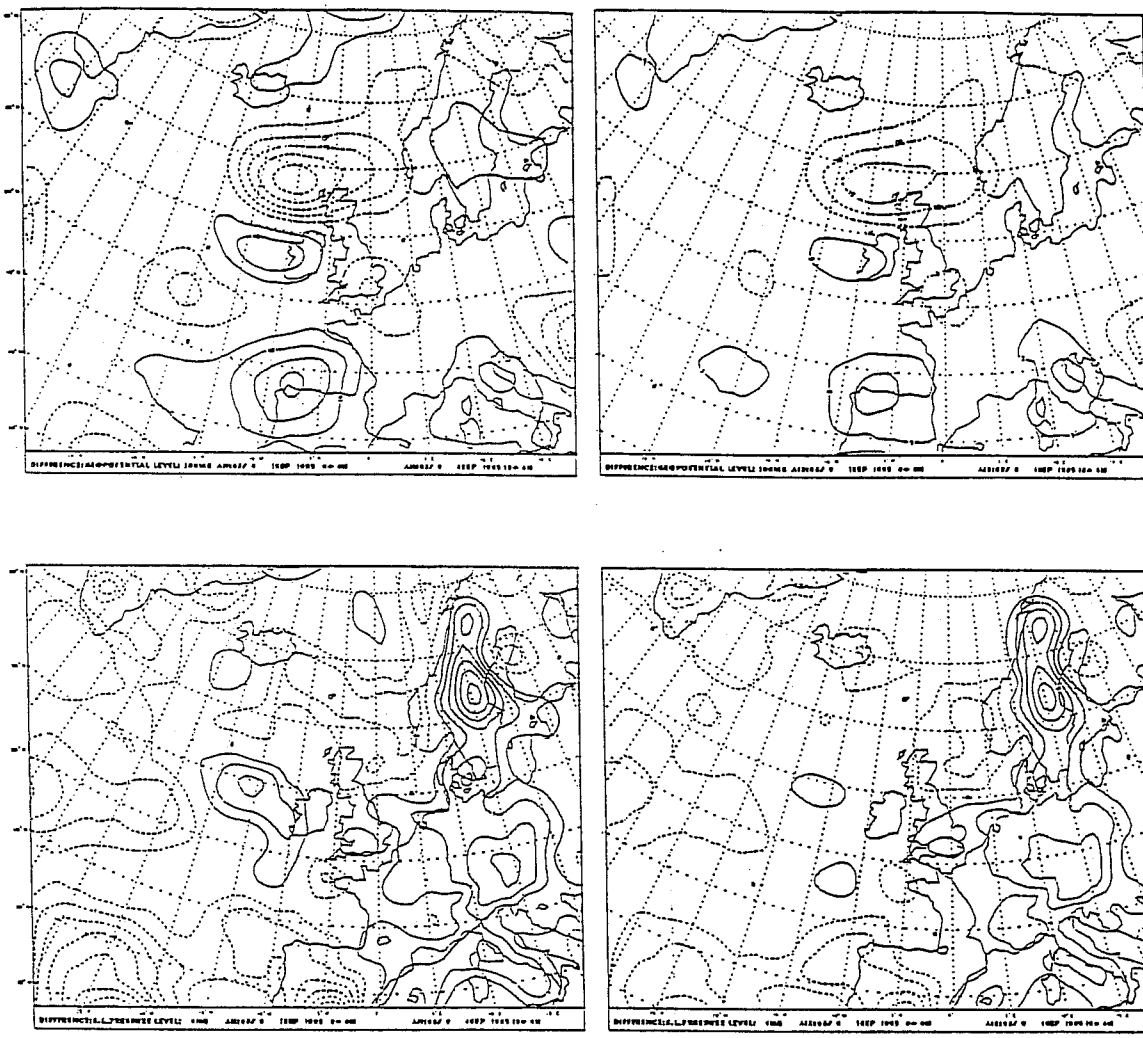

Differences between analysis and +6 h first guess forecast fields valid at 00 GMT 5 Sept 1985 for experiment A11. The 500 hPa geopotential height (above) and sea-level pressure (below). Contour intervals: 5 m for the 500 hPa height and 0.5 hPa for the sea-level pressure.

Differences between analysis and +6 h first guess forecast fields valid at 00 GMT 5 Sept 1985 for experiment A13. The 500 hPa geopotential height (above) and sea-level pressure (below).

Fig. 12 Analysis increments at 5 September 1985 00 UT for data-assimilations A11 (left) and A13 (right)

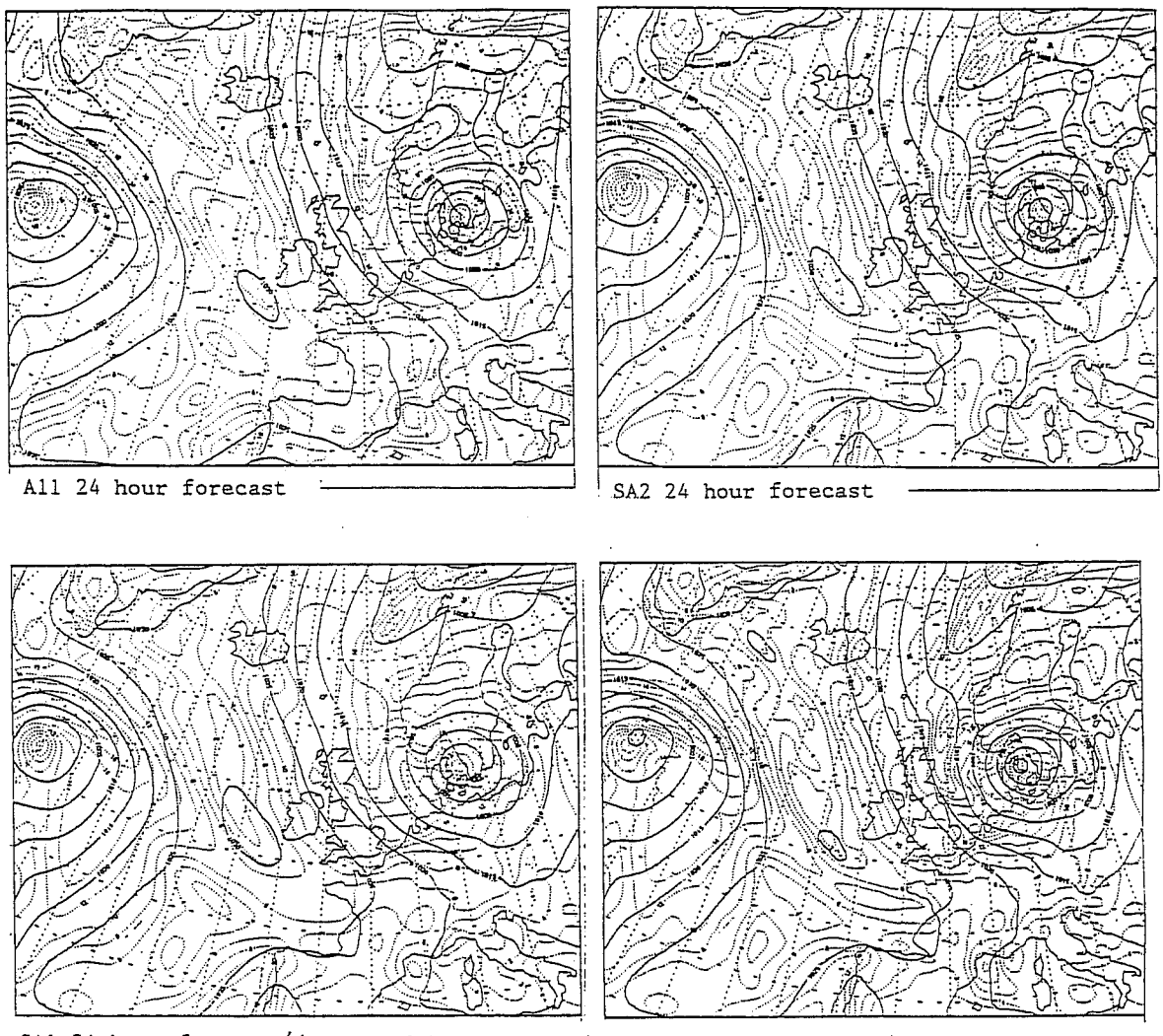

Fig. 13 Various HIRLAM baseline forecasts valid at 6 September 00 UT. MSL pressure contour intervals 5 hPa

sed by a factor of 2.5 compared to the standard values used in all previous assimilations.

The most important difference between this data-assimilation, SA1, and the A11 assimilation is probably the observational data bases used. In the A11 assimilation the operational data base at DMI was used, whereas the ECMWF observational data base was used in the SA1 assimilation. In this latter data base additional data are included, partly because it contains data received also after the operational cut-off times and partly because TOVS (SATEM) data are received at ECMWF with a 250 km resolution whereas only the 500 km resolution SATEMS from GTS are received at DMI. Actually, for the present period very little SATEMS were included in the DMI data base.

The 24 hour surface forecast with the standard baseline model, the SA2 forecast, is shown in Figure 13 together with the standard A11 forecast. Except for a slightly improved position the same verification scores (see Table 2) are obtained for the two forecasts. Figure 13 also shows a forecast, SA1, with increased horizontal diffusion (by a factor of 2.5) and one, SA3, with decreased horizontal diffusion (by a factor of 10). It is seen that the forecast depends very much upon the level of the horizontal diffusion. The SA3 forecast, with decreased horizontal diffusion, gives almost perfect verification scores for the low, whereas a clear dampening is seen in the SA1 forecast, with increased diffusion. The small scale noise is, however, not controlled sufficiently well in the forecast with the reduced diffusion.

The experiments clearly show the importance of the formulation of the horizontal diffusion, at least for explosive baroclinic developments as in the September case considered here. Therefore, it seems important to develop and test alternative formulations which more selectively control noise without a too severe dampening of the meteorologically significant developments.

3.3 Sensitivity to boundary fields

Due to computer restrictions the size of the integration area used in the present case study was limited. We tried to choose the geographical location of the area so that the important developments should be influenced as little as possible by the specified, time-dependent boundary fields. Furthermore, we tried to minimize the errors at the boundaries by the use of analyses as boundary fields.

In all experiments described in this note we use the simplified Davis boundary relaxation scheme, which originally was introduced and tested at ECMWF by Kållberg and Gibson (1977). The boundary fields used were given with 12 hour intervals between which linear interpolation in time was used. The initial baseline analysis was used as the boundary field at t = 0 and SMHI operational LAM analyses interpolated to the model grid were used at t = +12 h, +24 h, +36 h, ...

In order to see the effect of different boundary fields a 24 hour

forecast was made with initial data from the A11 analysis at 5 Sept. 00 UT and with boundary fields determined from the ECMWF forecast from 4 Sept. 12 UT. Difference fields between this forecast, A14, and the standard A11 (analysed boundaries) +24 h forecast are shown in Figure 14. It is seen that large differences have been "advected" into the area, in particular from the western and northern boundaries. The differences in boundary fields have, however, had only a minor impact on the development of the low over Southern Scandinavia in which we are in particular interested. The verification scores for the two forecasts (Table 2) are seen to be virtually the same.

3.4 Sensitivity to horizontal resolution

In order to see the impact of the horizontal resolution a data-assimilation and forecast experiment, L01, with half the resolution, i.e. with $\Delta\lambda' = \Delta\phi' = 1^{o}$, was performed. An early version of the baseline data-assimilation system was used in which full fields were interpolated from pressure to sigma surfaces instead of analysis increments, and in which the original SMHI non-linear balance equation was used instead of the non-linear normal mode initialization scheme. Also some errors and inconsistencies in the vertical interpolation routines had not yet been corrected. The L01 forecast should be compared with the high resolution forecast A04 which is based on initial data from a high resolution assimilation with the very same early data-assimilation system. It should be pointed out that all analysis parameters, including the forecast error correlation functions and the forecast error variances, were the same in the L01 and A04 analysis. Thus, the maximum resolution of the analysis increments was the same in the L01 and the A04 analysis.

The two 24 hour surface forecasts are shown together in Figure 15 (the verification scores are given in Table 2). As expected, the high resolution forecast yields a deeper low with a steeper pressure gradient, and thus higher wind speeds. The position of the centre is almost the same in the two forecasts. Note also the sharper frontal troughs in the high resolution forecast.

4. EXPERIMENTAL FORECASTS USING COMPONENTS OF THE HIRLAM LEVEL 1 SYSTEM

4.1 Sensitivity to vertical diffusion

The main difference between the baseline and the level 1 prediction model is the physical parameterization package.

The initial development and tests of the new package to be used in the level 1 model were carried out within the framework of the baseline model. Using initial data from a baseline data-assimilation, A09, in which the standard baseline prediction model has been used, the new parameterization schemes were introduced one by one in the baseline model and a forecast was made to see the impact. Results from these

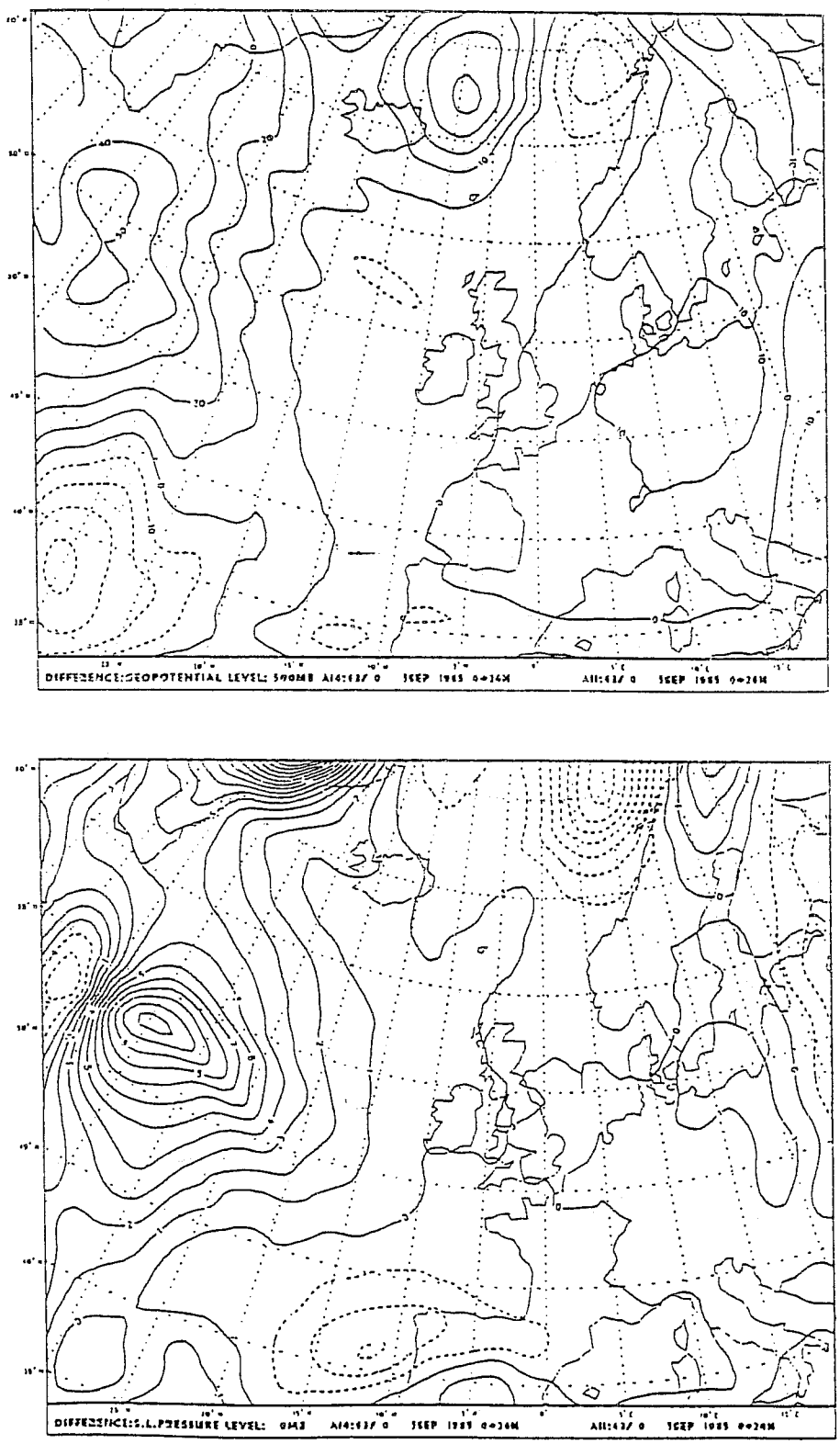

Fig. 14 Differences between two (A14 - A11) +24 h forecasts valid at 00 GMT 6 Sept 1985. The 500 hPa geopotential height (above) and sea-level pressure (below). Contour intervals: 10 m for the 500 hPa height and 1 hPa for sea-level pressure.

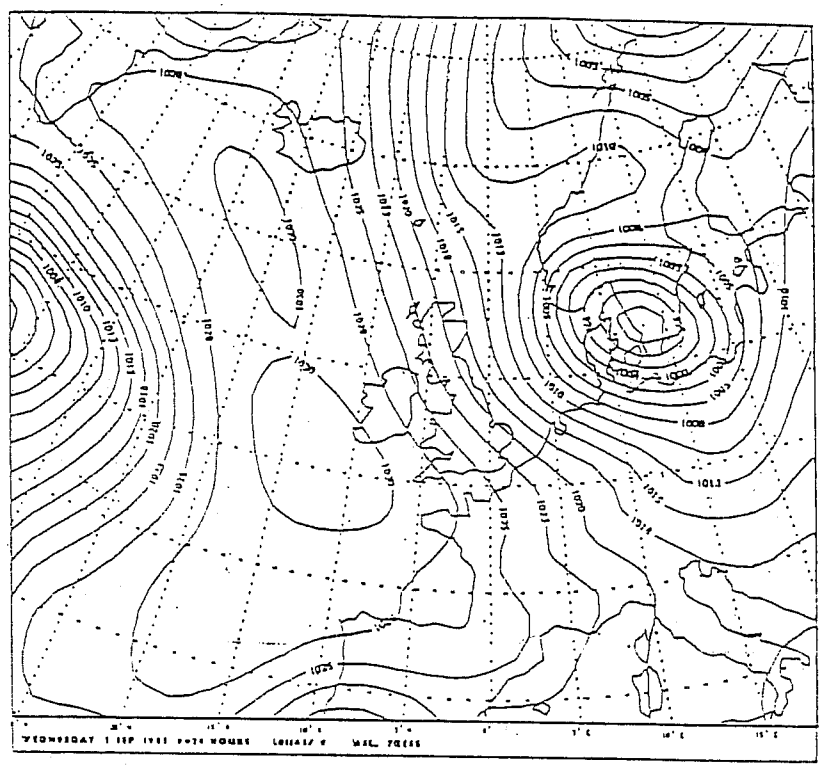

Low resolution forecast (L01)

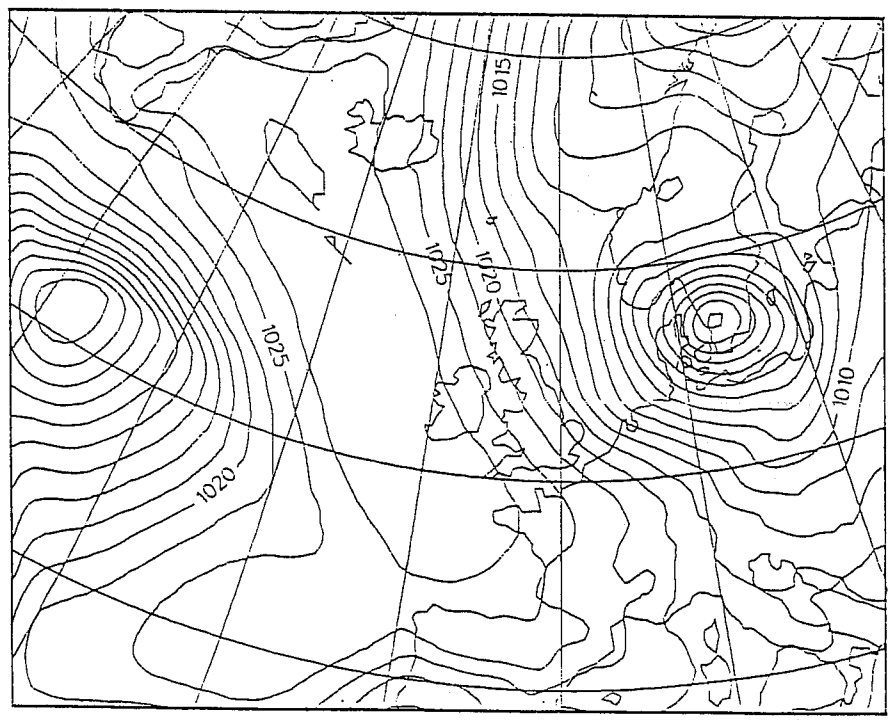

High resolution forecast (A04)

Fig. 15 24 hour baseline sea-level forecasts valid 6 September 1985 00 UT. MSL pressure contour intervals 2.5 hPa

initial tests of the new physical package are reported in Gustafsson et al. (1986). Here we shall bring only the results obtained in such experiments with the new vertical diffusion scheme.

The baseline analysis used as initial fields for these experiments were taken from a data-assimilation, A09, which differed from the A11 assimilation in that full field vertical interpolation was used from analysis levels to model levels and that the SMHI non-linear balance equation was used. The 24 hour surface forecast with the standard baseline model, the A09 forecast, is shown in Figure 16, together with two forecasts made with versions of the baseline model in which the new vertical diffusion scheme had been substituted instead of the baseline scheme.

The new HIRLAM vertical diffusion scheme is quite similar to the scheme used at present in the ECMWF T106 model. It deviates in two respects only. Firstly, virtual static energy is used instead of dry static energy in the Richardson number. Secondly, a simplified expression is used for the ratio between mixing lengths for dry static energy (l_s) and that for momentum (l_m).

The expression used in the HIRLAM scheme is

$$l_s/l_m = \lambda_s/\lambda_m \, [1-(1-\lambda_m/\lambda_s)\sigma^2]$$

where λ_s and λ_m are asymptotic mixing lengths and where we use, as in the ECMWF scheme, $\lambda_s/\lambda_m = 2.74$. Also, as in the ECMWF scheme,

$$l_s = \frac{kz}{1 + kz/\lambda_m}$$

where z is the height and k the von Karman constant.

In the first experimental forecast, F02, we used the value of λ_m which at present is used operationally at ECMWF, i.e. $\lambda_m = 160$ m. In Figure 16 and Table 2 it is seen that this leads to a significantly worse forecast. Especially, the central pressure was increased by 5 hPa compared to the baseline forecast A09. In the following experiment we tried a reduced value, $\lambda_m = 30$ m. The resulting forecast, F04, is seen to be very similar to the A09 forecast.

We believe that the poor result of the F02 forecast with $\lambda_m = 160$ m, was caused by a weakening of the baroclinic mass and wind fields due to a too vigorous vertical diffusion. This was confirmed also by experiments with a 16 level one-dimensional version of the forecast model in which a severe smoothing of an initial jet profile was observed already after 24 hours, when $\lambda_m = 160$ m was used. As a value of λ_m of the order of 30 m corresponds more closely to empirically determined values of the mixing length (i.e. Blackadar (1962)), we have initially chosen that value for the HIRLAM level 1 scheme.

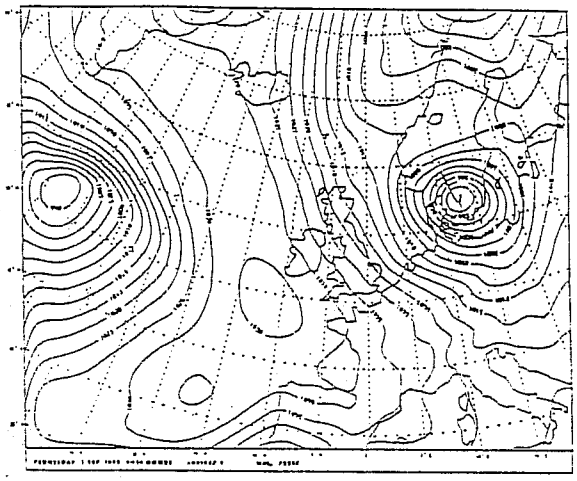

A09 baseline forecast

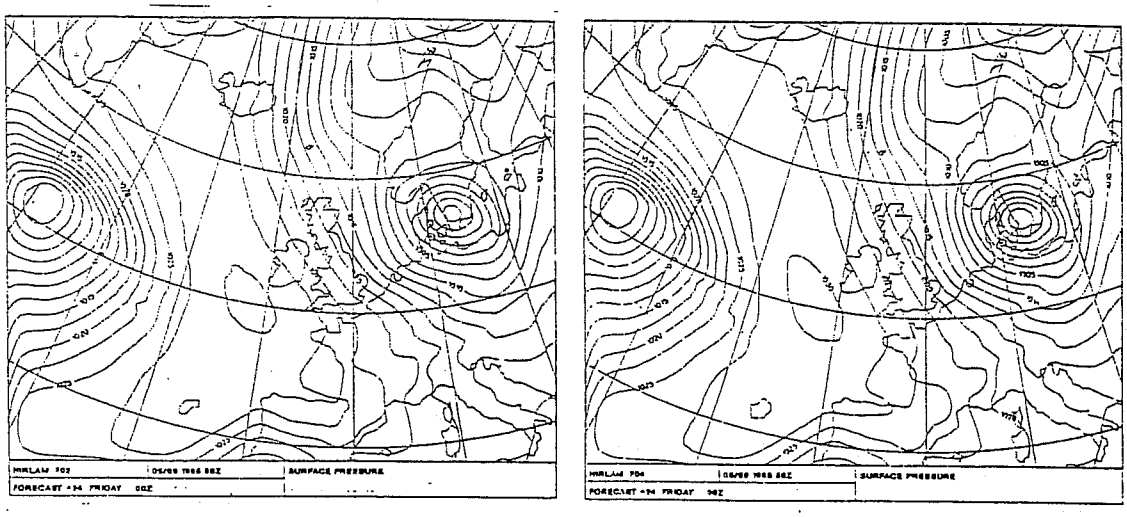

λ_m = 160 m. λ_m =30 m

Baseline forecasts F02 (left) and F04 (right) with upgraded vert. diffusion

Fig. 16 24 hour sea-level forecasts valid 6 September 1985 00 UT.
MSL pressure contour intervals 2.5 hPa.

4.2 Impact of new analysis scheme

In order to see the difference between the baseline and the level 1 analysis schemes we made a data assimilation/forecast experiment AA8, in which the new analysis scheme (and the new initialization scheme) were used together with the baseline model. Otherwise the experiment is similar to the SA2 forecast with the SA1 initial fields in which the baseline analysis and initialization schemes were used. The resulting AA8 forecast is shown in Figure 17 together with the SA2 forecast. It is seen from the verification scores in Table 2 that the level 1 analysis scheme gives a significant improvement in the forecast of the low over Denmark.

Several more experiments were made with the level 1 analysis scheme and reported in Gustafsson and Järvenoja (1987). It is obvious that further development and tuning of the structure functions and the data selection scheme is needed, but results obtained so far indicate that the limited area version of the ECMWF analysis scheme is indeed a good selection as a basis for the HIRLAM analysis scheme.

4.3 Impact of the new prediction model

As described above the main difference between the baseline and the level 1 prediction model is in the physical parameterization package. Two forecasts with different versions of the level 1 model are presented in Figure 18. The initial data used for both forecasts were from the data-assimilation AA8 described in the preceding sub-section.

The NT1 forecast, shown to the left, is made with the heating/cooling due to radiation turned off in the free atmosphere. Thus, it includes radiation effects only at the surface and is in this respect similar to the baseline forecast AA8. The NT1 forecast is the very best of our forecasts made so far. Compared to the forecast AA8 a 2 hPa deeper central pressure and a larger pressure gradient SW of the low is obtained in this forecast with the level 1 model. Figure 19 is shows the surface map of the forecast together with the verifying DMI hand analysis. It is obvious that this forecast would have been an excellent guidance for the forecasters on duty.

The NT2 forecast, which is also shown in Figure 18, is made from the same initial data (AA8) as the NT1 forecast, but here the full radiation scheme is included in the forecast model. From Table 2 it is seen that similar verification scores are obtained for the NT2 and NT1 forecasts except that the central pressure is 2 hPa higher than in the NT1 forecast. As seen in Figure 20 this difference is due to a rather uniform increase of the pressure over the whole integration area in the NT2 forecast. Supported by some additional experiments we believe that the spurious inflow of mass over the boundaries of the integration area, which is causing the increase in surface pressure, is due to the difference between the baseline prediction model used in data-assimilation AA8 and the level 1 model version used in the NT2 forecast. The baseline model used to obtain first guess fields in the AA8 data-assi-

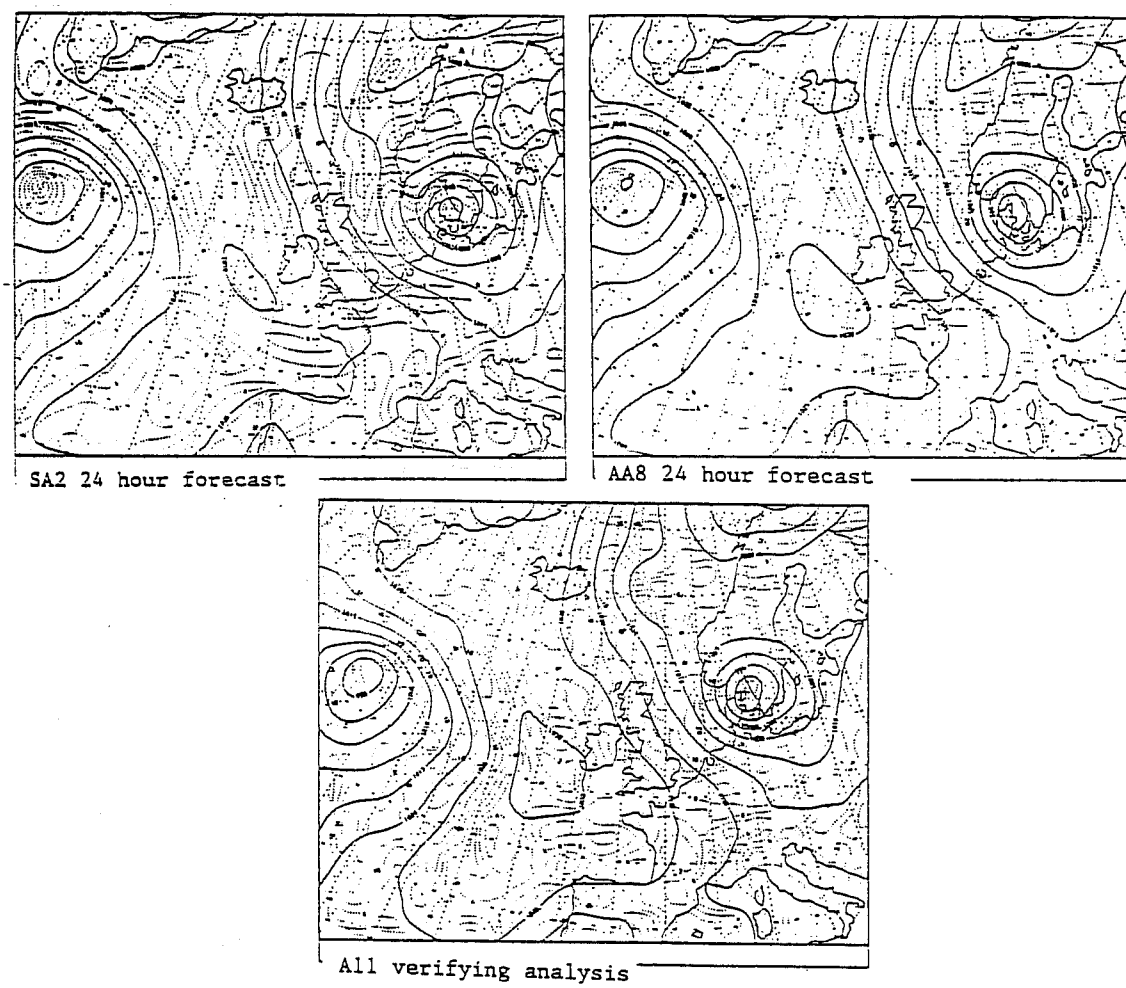

Fig. 17 HIRLAM baseline 24 hour forecasts with baseline initial analysis (SA2) and level 1 initial analysis (AA8), together with verifying baseline analysis valid at 6 September 1985 00 UT. MSL pressure contour intervals 5 hPa

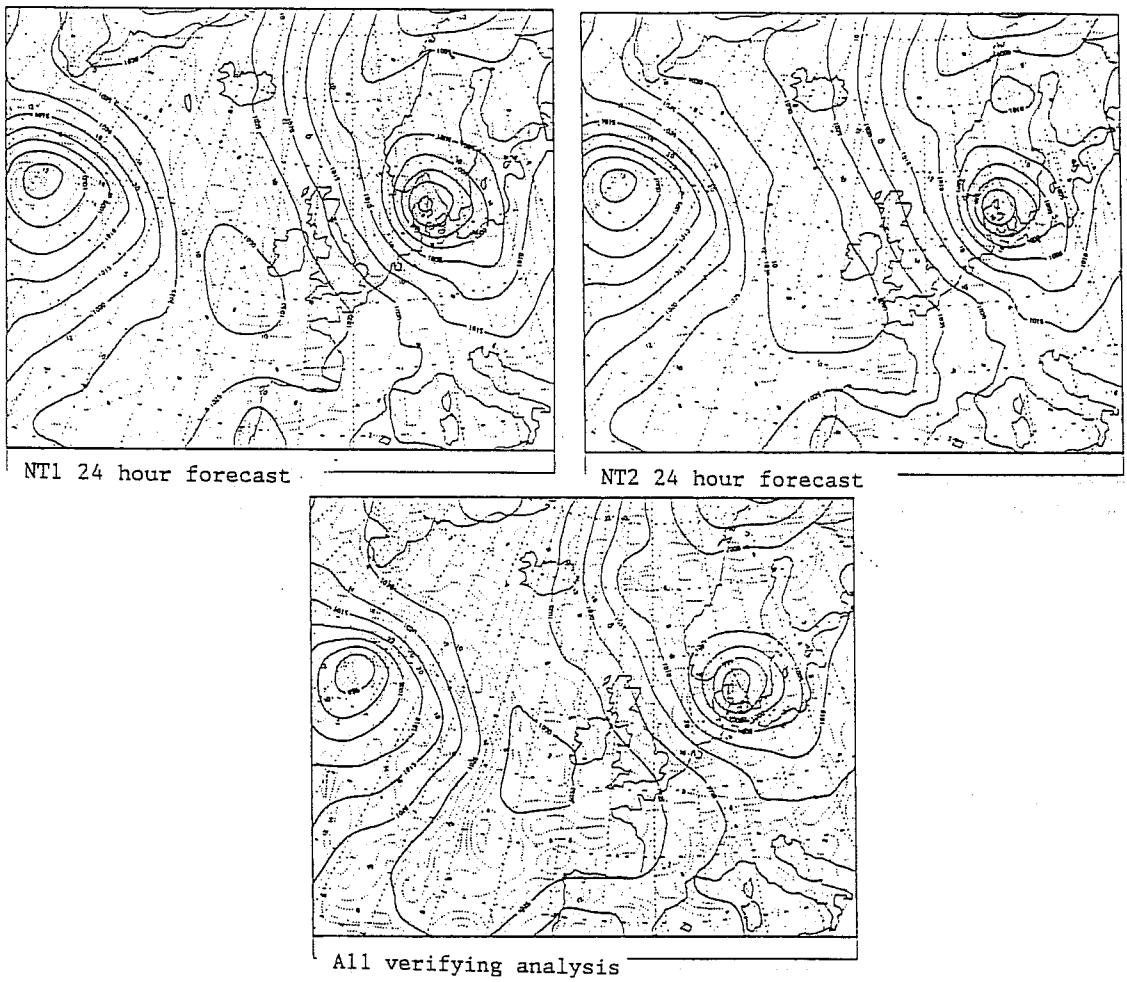

Fig. 18 HIRLAM level 1 24 hour forecasts together with verifying baseline analysis valid at 6 September 1985 00 UT. MSL pressure contour intervals 5hPa

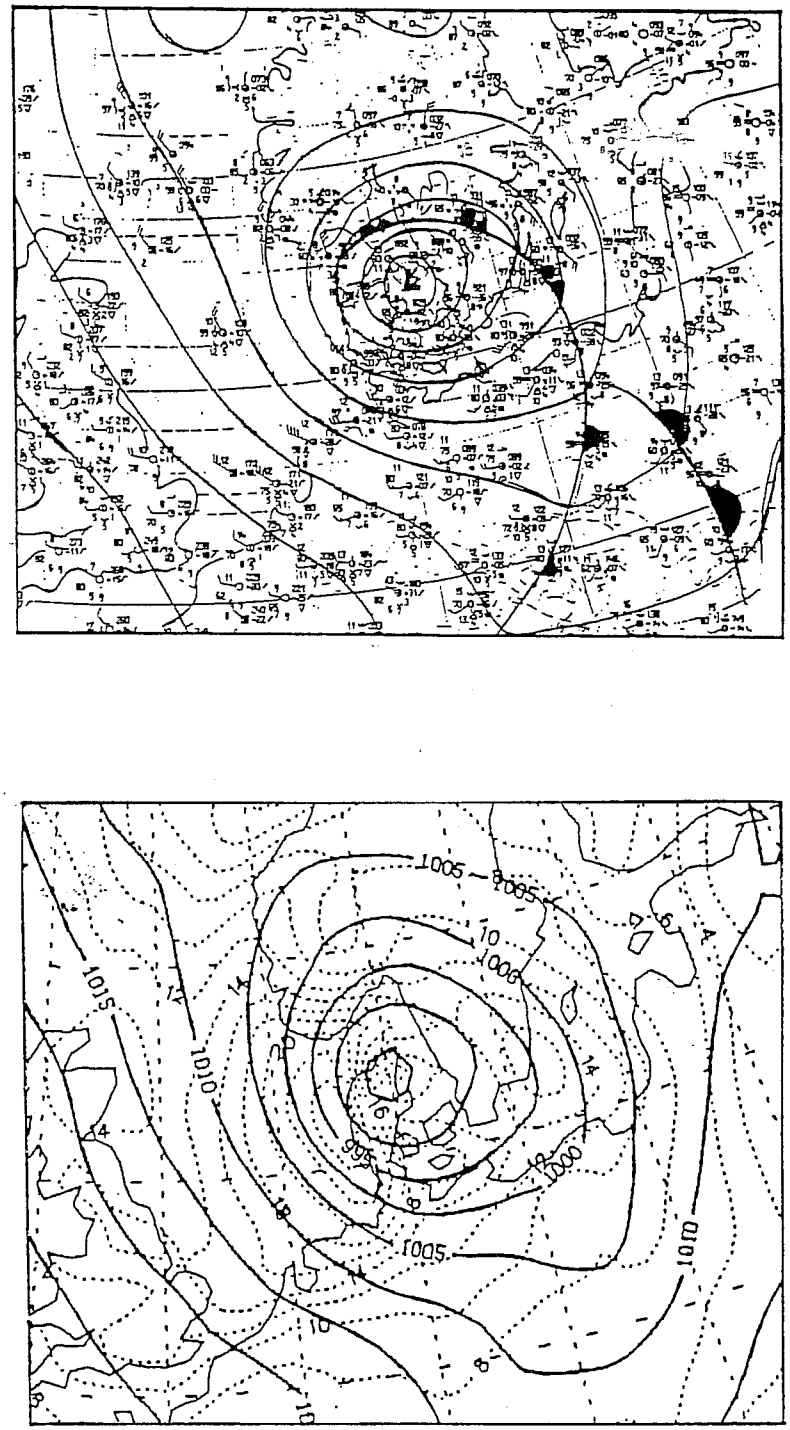

Fig. 19 DMI surface hand analysis (above) and HIRLAM level 1 (NT1) 24 hour sea-level pressure forecast (below). Contour intervals 5 hPa

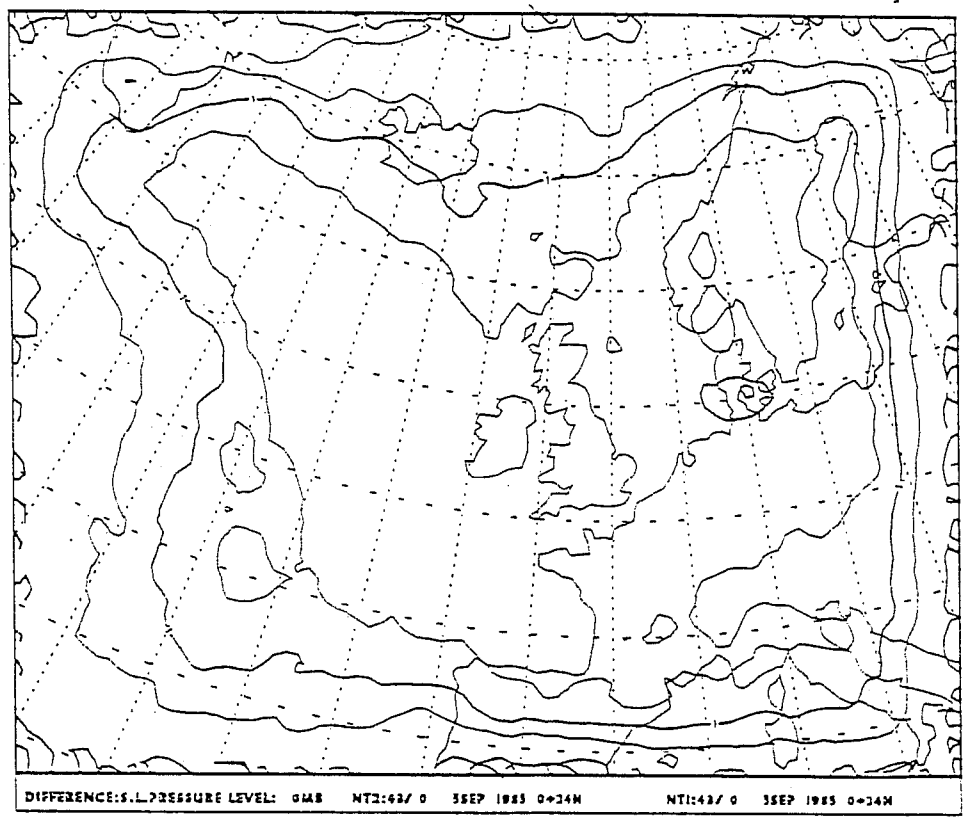

Fig. 20 Difference in sea-level pressure between the two 24 hour forecasts NT2 and NT1 (NT2-NT1). Contour intervals 0.5 hPa.

milation does not include radiational effects in the free atmosphere. Therefore we believe that the temperature fields in the analysis are too warm. When a forecast is then made with the level 1 model which includes radiational effects and which uses the too warm initial analysis as the first boundary field then the radiational cooling over the integration area leads to an inward directed pressure gradient in the boundary zone, which in turn causes the spurious mass inflow. If our suspicions are correct we should expect that the problem will be solved when the level 1 model including all radiation effects is used in the data-assimilation, as well as in the subsequent forecast.

5. CONCLUDING REMARKS

In the foregoing results of data-assimilation and forecasts of an explosive deepening cyclone were reported. Sensitivity of the forecasts to several of the system components was demonstrated. The sensitivity to the initial state and thereby to the observational data and the choise of analysis parameters was clearly demonstrated.

The limitation of predictability due to an insufficient data coverage over the Atlantic Ocean in the case considered points at the need for additional observations or an improved utilization of available data. Realising that no substantial improvements in the coverage of conventional observations will take place in the near future it will be of the utmost importance to make the full use of high resolution satellite data, particularly over the oceans.

Also sensitivity to model formulation in particular horizontal resolution, horizontal and vertical diffusion and an improved physical parameterization were demonstrated.

The performance of an initial HIRLAM baseline system was compared with a more up-to-date experimental HIRLAM level 1 system and each of the main components of the latter system was shown to give improved short--range forecasts of the explosive development considered.

During the remaining year of the HIRLAM project, at first some minor upgradings of the level 1 system will be made before the start of the pre-operational tests of the system at the beginning of 1988.

In parallel with the pre-operational tests further developments and tests of different components of the system are planned. The most important further developments planned are utilization of high resolution TOVS data, diabatic non-linear normal mode initialization, the introduction of a semi-Lagrangian time scheme and a cloud/condensation scheme including cloud liquid water in the prediction model.

With the planned upgradings we hope at the end of the project period to have a HIRLAM system with further improved forecast capabilities as regards general short-range forecasting and in particular forecasting of explosive developments as the September case considered here.

REFERENCES

Andersson, E., L. Meuller, N. Gustafsson and G. Omstedt, 1986: Development of Meso-scale analysis schemes for nowcasting and very short-range forecasting. SMHI PROMIS-rapporter, No. 1. 41 pp + Appendix.

Bijlsma, S.J. and L.M. Hafkenscheid, 1984: A non-linear normal mode initialization method for a limited area model. Internal KNMI Note, 38 pp.

Blackadar, A.K., 1962: The vertical distribution of wind and turbulent exchange in a neutral atmosphere. J. Geophys. Res. 67, 3095-3102.

Gustafsson, N., S. Järvenoja, P. Källberg and N. Woetmann Nielsen, 1986: Baseline experiments with a high resolution limited area model. HIRLAM Technical Report No. 1, 87 pp.

Gustafsson, N. and S. Järvenoja, 1987: Sensitivity tests with the limited area version of the ECMWF analysis scheme. HIRLAM Technical Note No. 3, 26 pp.

Källberg, P.W. and J.K. Gibson, 1977: Lateral boundary conditions for a limited area version of the ECMWF model. WGNE Progress Report No. 14. WMO Secretariat 103-105.

Lönnberg, P. and A. Hollingsworth, 1986: The statistical structure of short-range forecast errors as determined from radiosonde data. Part II: The covariance of height and wind errors. Tellus, 38A, 137-161.

Machenhauer, B., 1977: On the Dynamics of Gravity Oscillations in a Shallow Water Model, with Applications to Normal Mode Initialization. Beitr. Phys. Atmos. 50, 253-271.

Nordeng, T.E. and A. Foss, 1987: Simulations of storms within the HIRLAM baseline experiment with the Norwegian mesoscale limited area model system. HIRLAM Technical Report No. 2, 22 pp.

Rattenborg, M., 1986: Normal mode initialization on a limited area. Masters thesis, Univ. of Copenhagen, 142 pp. (In Danish).

Undén, P., 1982: The Swedish Limited Area Model. SMHI Reports, Meteorology and Climatology, RMK 35, 33 pp.